N69-30871
(ACCESSION NUMBER)

67
(PAGES)

NASA CR-101745
(NASA CR OR TMX OR AD NUMBER)

(THRU)

1
(CODE)

33
(CATEGORY)

FACILITY FORM 602

THERMO ELECTRON

CORPORATION

Report No. TE 5045-145-69

HYDROGEN-OXYGEN FIRED THERMIONIC GENERATORS AND THERMIONIC DIODES

3 April 1969

Contract NAS 9-4282

Prepared for

NASA Manned Space Flight Center
Houston, Texas

Thermo Electron Corporation, 85 First Avenue, Waltham, Massachusetts 02154

TABLE OF CONTENTS

LIST OF ILLUSTRATIONS

LIST OF ILLUSTRATIONS (continued)

LIST OF TABLES

I. INTRODUCTION AND SUMMARY

The program described herein was undertaken to provide hardware with which to evaluate the state-of-the-art of thermionic flame-heated devices for use in a short (a few hours to a few days) space mission. The reactants available as fuel and oxidant in the mission were expected to be hydrogen and oxygen, and these same reactants were employed in the program.

In the program two hydrogen-oxygen 50 watt generators were built and delivered, as were two spare thermionic diodes.

Although the generators were successfully operated, their efficiency was far below that initially expected. Self-bonded silicon carbide was the only material available that could resist the high temperatures and the thermal shock. This material was found highly permeable to hydrogen, and this precluded the design of a truly efficient combustor.

Use of vapor-deposited silicon carbide, either free-standing or as a coating, is recommended as a way of circumventing the above difficulty in future such devices.

A. COMBUSTOR DESIGN

The goal of the combustor design was to employ as much as possible the features of the natural gas-air combustor that had been developed earlier. Changes were limited to those deemed necessary to accommodate the reactants (hydrogen and oxygen) and to maximize burning efficiency with these reactants.

Because the thermionic diode must operate at a relatively high emitter temperature (> 1300°C) to achieve good performance, recuperation of energy from the products of reaction was judged necessary to prevent loss of the bulk of the fuel's energy in the exhaust. A three-stage baffled-type recuperator was therefore employed in the exhaust gas path to preheat the incoming hydrogen.

In the stoichiometric hydrogen-oxygen reaction, two moles of hydrogen combine with one mole of oxygen; thus, greater energy utilization can be achieved by preheating the fuel rather than the oxidant.

The hydrogen-oxygen reaction when burning stoichiometrically produces an extremely high adiabatic flame temperature. Thus, a means was needed for gradually mixing the fuel and oxidant while simultaneously rapidly releasing heat in order to maintain the temperature of the combustion products within safe limits. As will be shown, all of the hydrogen was injected simultaneously, but the oxygen was added in stages to control the burning rate.

A small amount of excess hydrogen, 20%,was deemed necessary to maintain a rich mixture and preclude explosive reactant mixtures.

To achieve maximum efficiency in the transfer of heat from the fuel to the diode, the entire combustor was covered with high temperature thermal insulation. In turn, this reduction in heat transfer caused some of the combustion chamber parts to operate at very high temperatures. Self-bonded silicon carbide was deemed the only material suitable for these parts. It combines high temperature strength and oxidation resistance with excellent resistance to thermal shock. In one case a long, small-diameter tube was needed which was not available in silicon carbide, and aluminum oxide was used instead. Because of the small diameter, the part adequately resisted thermal shock.

The diode output requirement was 50 watts and diode efficiency was estimated to be 10%. Thus, at least 500 thermal watts were deemed necessary to drive the diode.

Figure I-1 shows the final design of the combustor. A ring of orifices was used to direct hydrogen into the region around the thermionic diode's hemispherical emitter. Oxygen passed through several rings of additional orifices, mixed with the hydrogen and burned. The oxygen from the ring closest to the incoming hydrogen reacted first, and subsequently oxygen from the more remote rings of orifices. The exhaust products then entered the first stage of a three-stage recuperator. Most of the high-temperature parts employed in the combustor were modifications of parts used in a gas-air combustor built earlier.

The silicon carbide orifice plate, Part #6, was enclosed by a concentric, larger silicon carbide cover, Part #8, to form an oxygen manifold. Oxygen entered the manifold via a small aluminum oxide tube, Part #10, that was spring-loaded against the manifold cover. Ground joints were employed to minimize leakage.

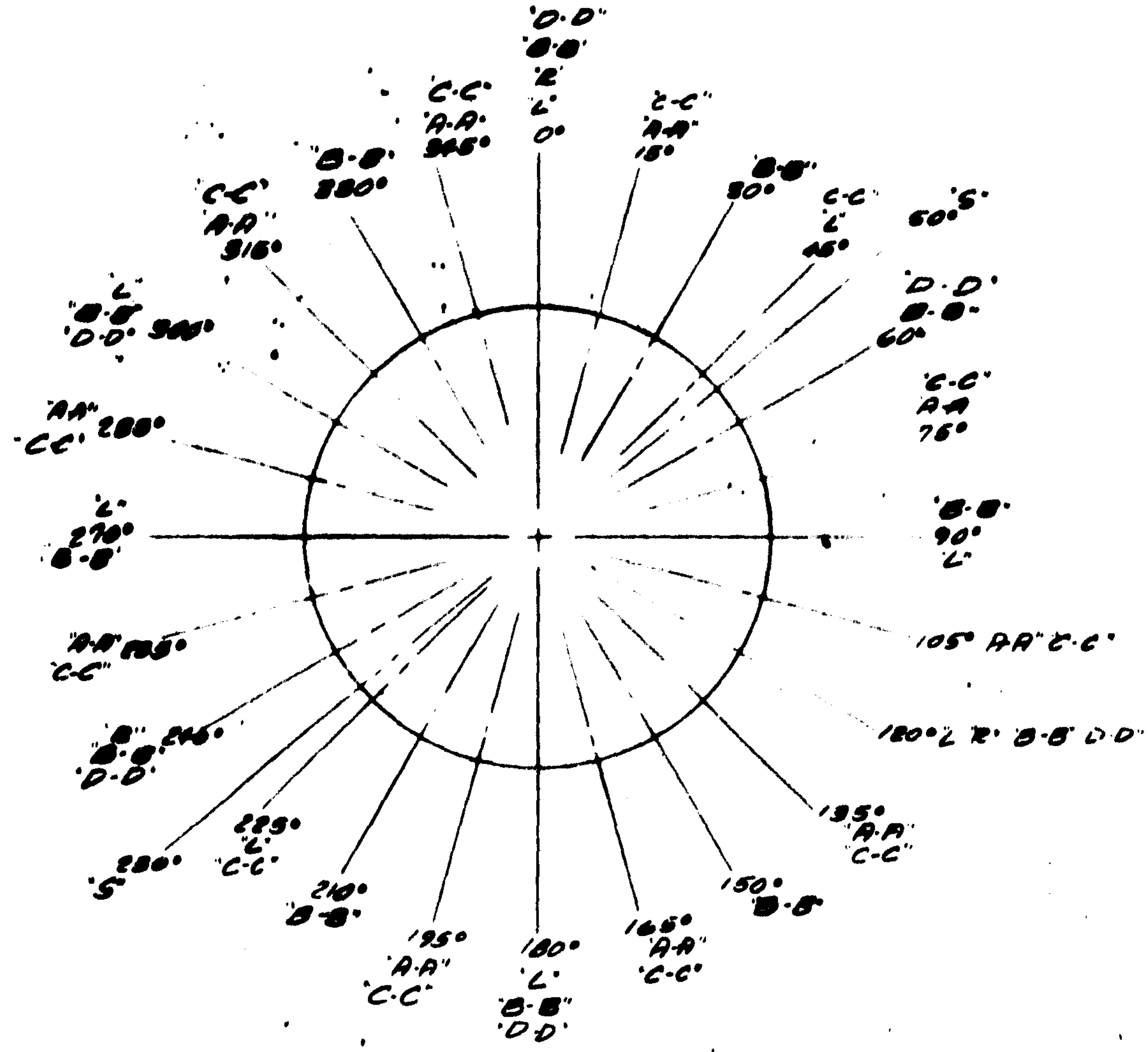

VIEW T-T
(FOR ORIENTATION ONLY)

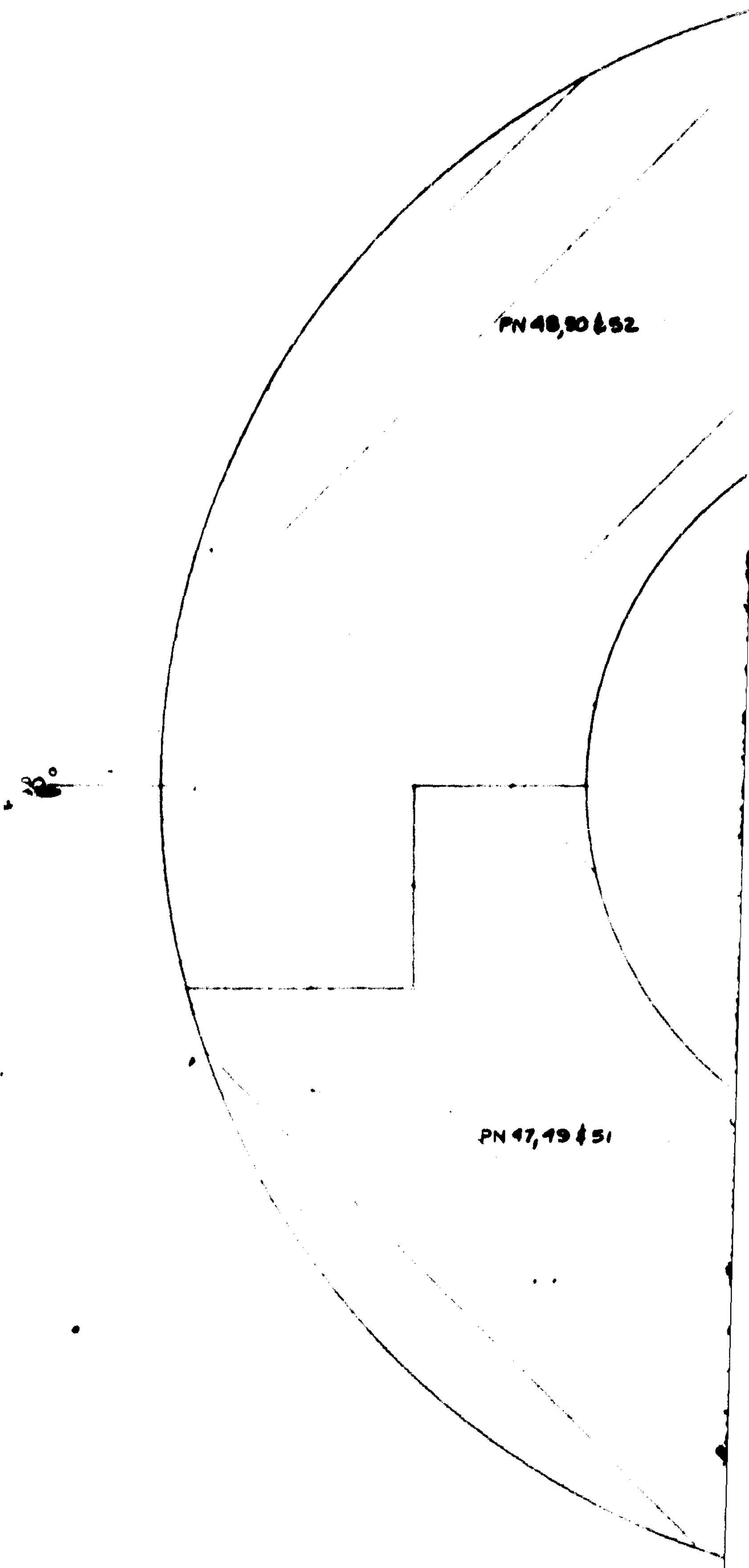

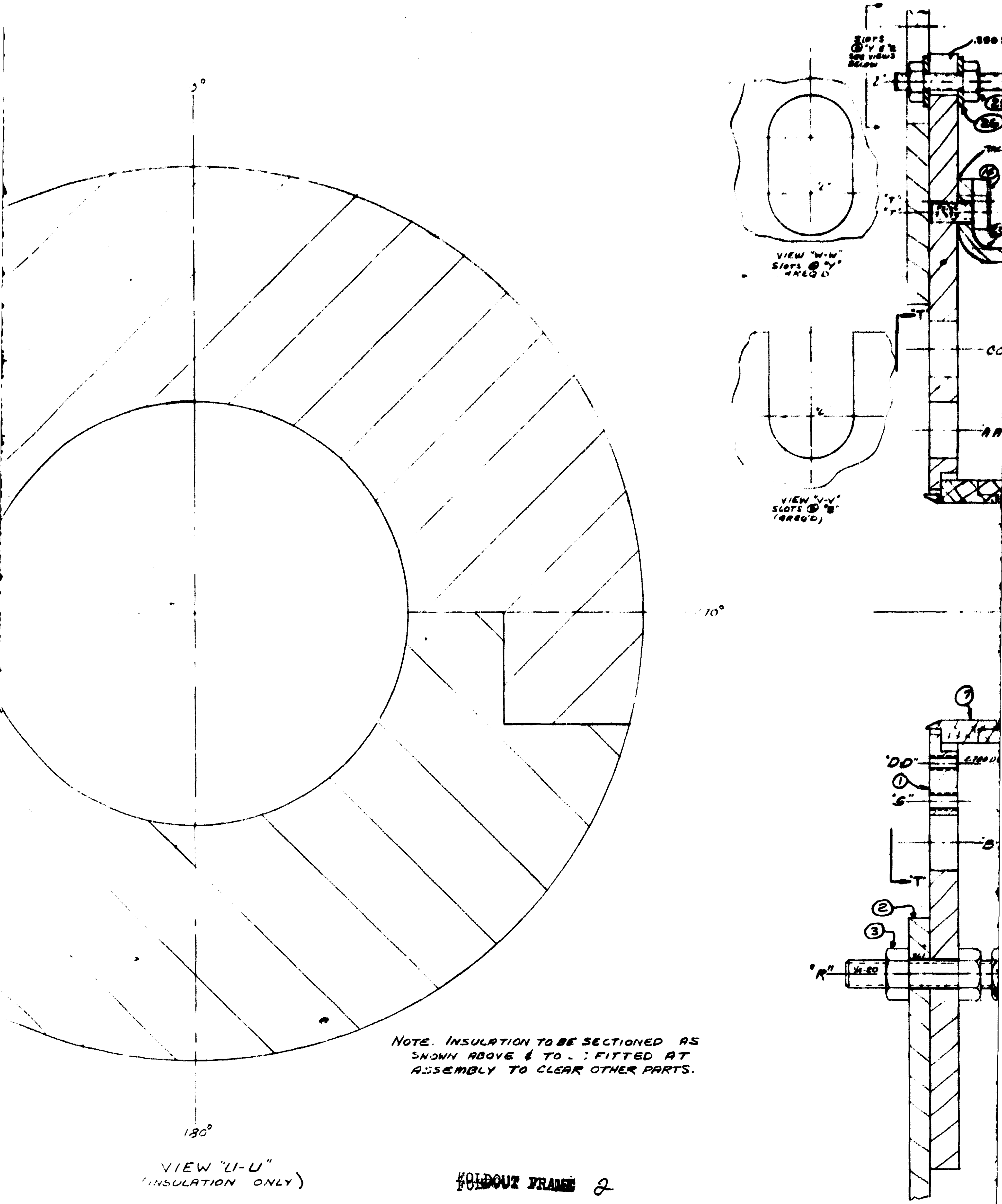
0°
90°
180°
VIEW "U-U"
(INSULATION ONLY)
NOTE. INSULATION TO BE SECTIONED AS SHOWN ABOVE ℄ TO . : FITTED AT ASSEMBLY TO CLEAR OTHER PARTS.
VIEW "W-W"
SLOTS @ "Y"
VIEW "V-V"
SLOTS @ "B"
(4 REQ'D)
"T"
"DD"
"S"
"R"
1/4-20

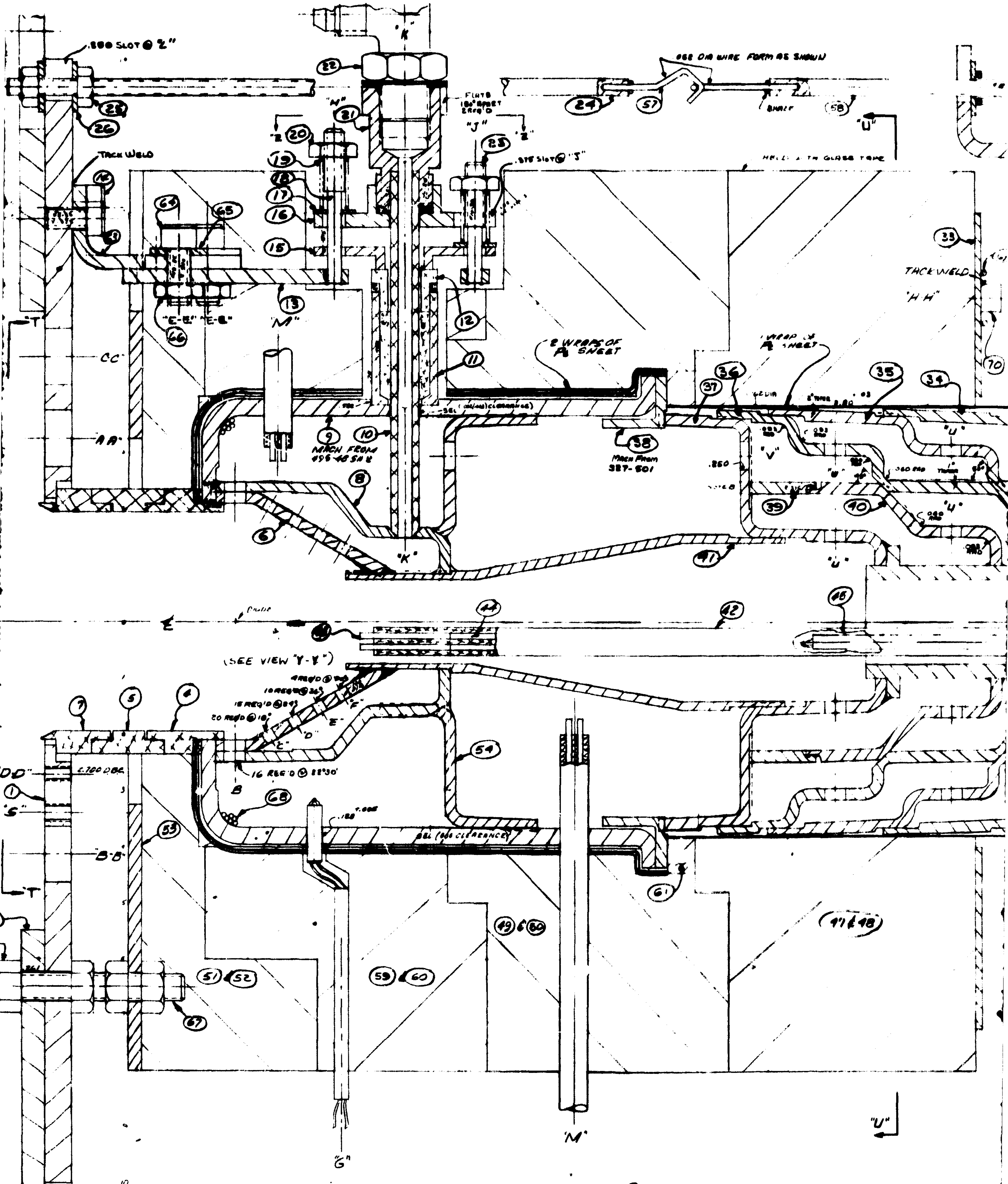

FOLDOUT FRAME 3

REV	DESCRIPTION	DATE	BY	APPR
A	SEE OBS LAYOUT (8-30-68)	[illegible]	[illegible]	
B	SEE OBS LAYOUT (3-25-67)	[illegible]	[illegible]	

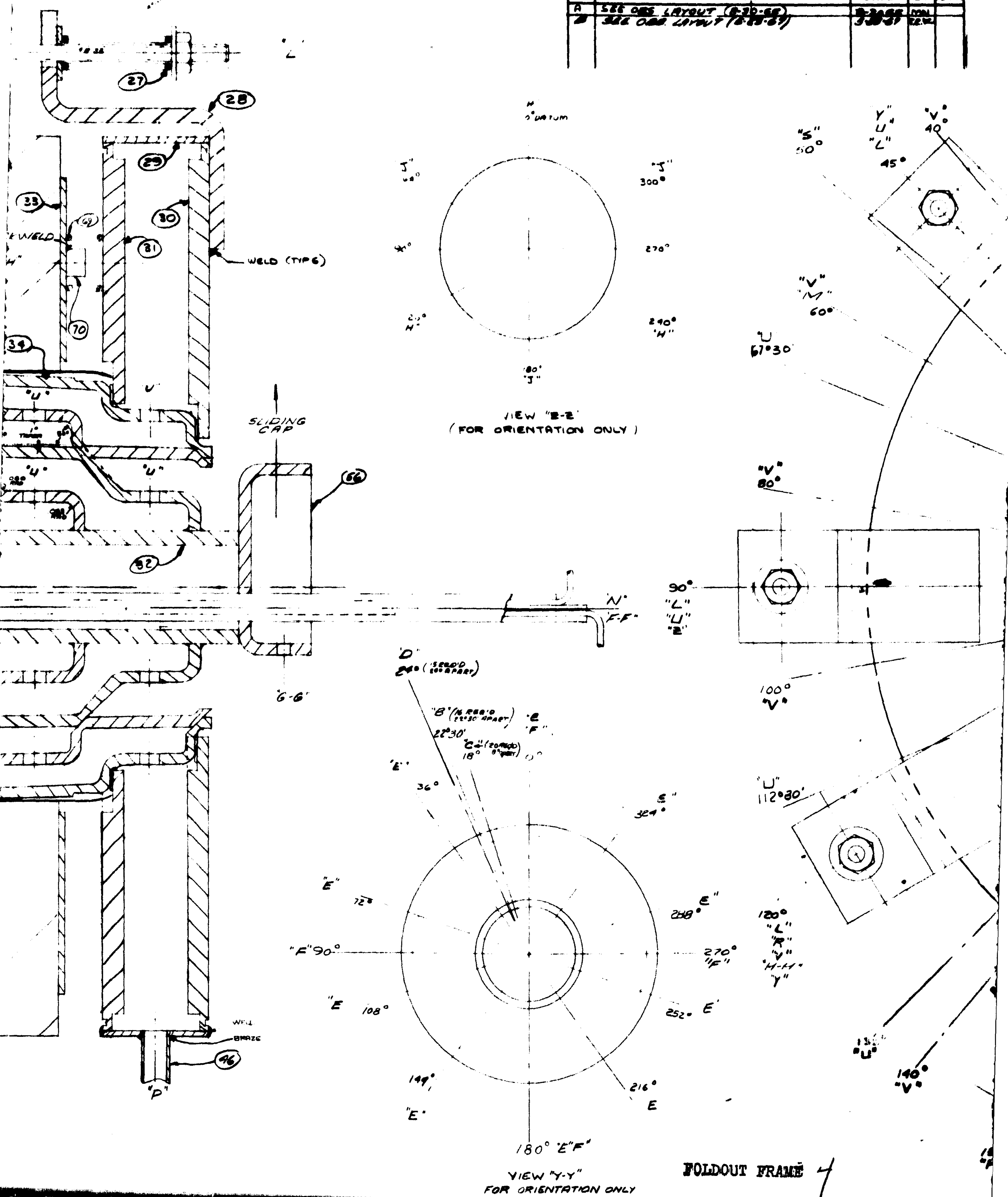

FOLDOUT FRAME 4

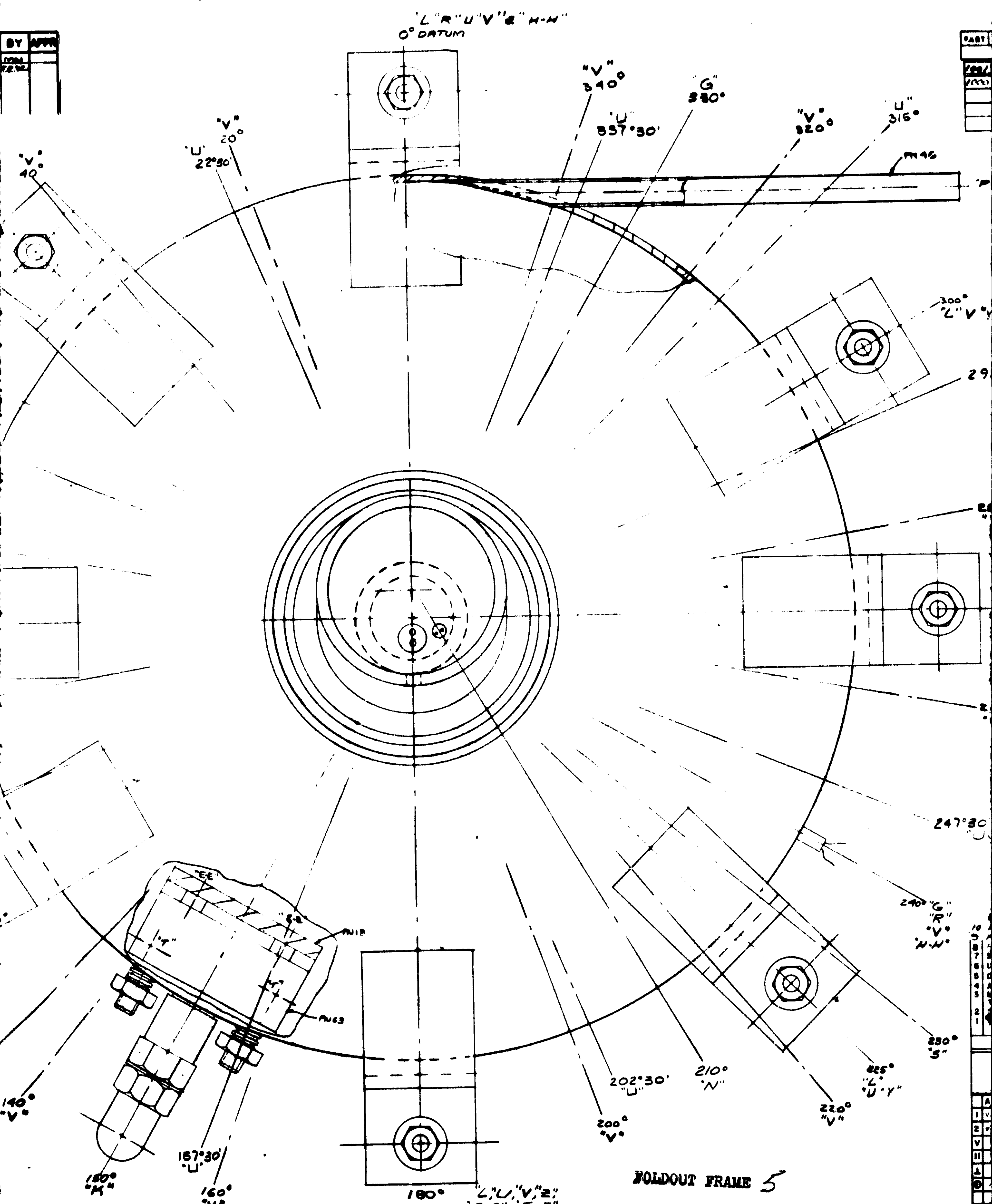

FOLDOUT FRAME 5

PART	SIZE	REQ			NOTES
LAYOUT & SUB ASSEM					
1001	D				PN 29, 30, 31 & 46 WELD'FM
1000	H			SHEET 2	OUTER CAN FOR VACUUM SHIELD

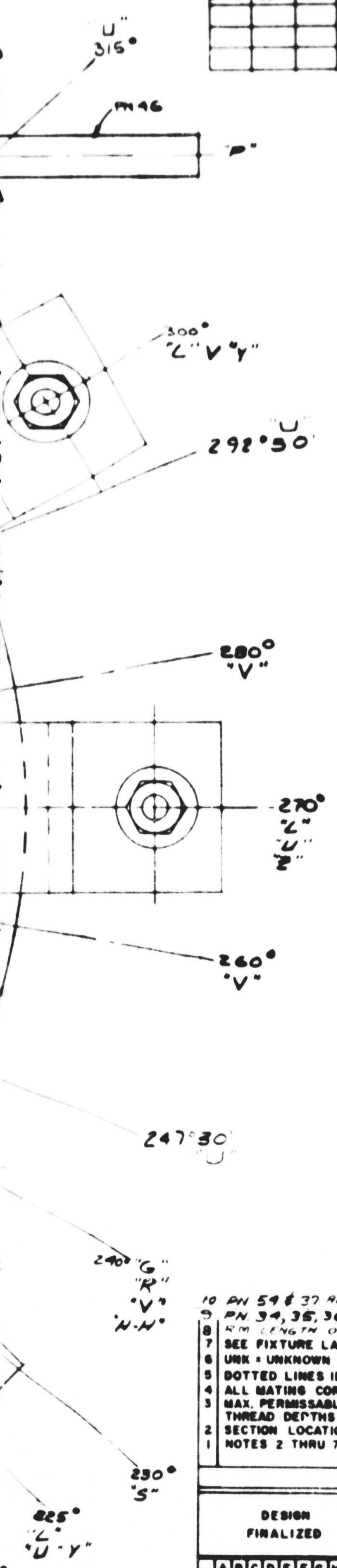

Figure I-1.
Hydrogen-Oxygen
Combustor - Final
Design

10	PN 54 & 37 ARE MADE FROM THE SAME CASTING
9	PN 34, 35, 36, 40, & 8 ARE MADE FROM THE SAME CASTING
8	RM LENGTH OF PN 39 = 5.500
7	SEE FIXTURE LAYOUTS (3090, 3190 ETC.) FOR FIXTURE INFORMATION.
6	UNK = UNKNOWN N.D = NO DRAWING, PROCURE FROM THIS L.O.
5	DOTTED LINES INDICATE ROUGH OR PRELIMINARY MACHINING.
4	ALL MATING CORNERS & FILLETS ARE .015 X 45° CHFR. AND .010 R. RES.
3	MAX. PERMISSABLE TAP DRILL DEPTH AND MIN. PERMISSABLE FULL THREAD DEPTHS ARE SHOWN.
2	SECTION LOCATIONS DEFINED BY LETTER LOCATION AT END VIEW.
1	NOTES 2 THRU 7 APPLY UNLESS OTHERWISE SPECIFIED.

NOTES

DESIGN FINALIZED	DATE	INT.	DATE	INT.	DATE	INT.	DATE	INT.

	A	B	C	D	E	F	G	H	J	K	L	M	N	P	R	S	T	U	V	W	Y	Z
1	✓	✓	✓	✓	✓	✓	✓	✓	✓	✓	✓	✓	✓	✓	✓		✓	✓	✓		✓	✓
2	✓	✓	✓	✓	✓	✓	✓	✓														
V																	✓	✓	✓	✓	✓	✓
II																						
⊥																						
◎																						

PART	SIZE	REV	REQ	MAT'L	NOTES
70	A		3	SS	
69	ND		3	SS	LC-0386-1 LEE
68	ND		6	Pt	.010 DIA.
67	ND		3	SS	1/4-20 x 2" LG THREADED ROD
66	ND		2	S.S.	#10-32 HEX JAM NUT
65	ND		2	S.S.	#10-32 PLAIN WASHER
64	ND		2	S.S.	#10-32 x .500 LNG S.H.C.S.
63	B		1	INCONEL	
62	B		1	S.S.	ALTERNATE INLET
61	B		1	DYNA-Q	INSULATION
60	D		1	DYNA-Q	INSULATION
59	D		1	DYNA-Q	INSULATION
58	B		8	SS	#8-32 THREADED ROD
57	ND		16	SS	.062 DIA WIRE
56	B		1	SiC	
55	ND		1	Pt	.003 THK
54	C		1	S.C	
53	D		1	INCONEL	
52	D	B		DYNA-Q	INSULATION
51	D	B		DYNA-Q	INSULATION
50	D			DYNA-Q	INSULATION
49	D			DYNA-Q	INSULATION
48	D		1	DYNA-Q	INSULATION
47	D		1	DYNA-Q	INSULATION
46	B		1	S.S.	
45	ND.		3	Al_2O_3	.125 O.D. 2 HOLE
44	ND		6	INCO	
43	ND		6	S.C	(KT)
42	C		3	Al_2O_3	.250 O.D. 2T .062 [illegible]
41	C		1	S,C	
40	C	A	1	S,C	
39	B/B		1	S,C	
38	D	A	1	S,C	
37	D/D	A	1	S,C	
36	D	A	1	S,C	
35	D	A	1	S,C	
34	C		1	S,C	
33	D		1	S.S.	
32	B		1	S.C	
31	C		1	S.S.	
30	C		1	S.S.	
29	D		1	S.S.	
28	C		8	S.S.	
27	ND		8	S.S.	SPRING LEE CAT. #LC-045D-15
26	ND		32	S.S.	#8-32 WASHER
25	ND		24	S.S.	#8-32 HEX NUT
24	B		8	S.S.	#8-32 THREADED ROD
23	A		3	S.S.	
22	ND		1	S.S.	PARKER #4C5BX-SS
21	B		1	S.S.	
20	ND		6	S.S	#10-32 HEX NUT
19	ND		6	S.S	SPRING LEE CAT. #LC-022C-3
18	A		3	S.S	
17	ND		6	S.S	#6-32 WASHER
16	B		1	S.S.	
15	B		1	INCONEL	
14	ND		2	S.S.	#8-32 x .375 LNG S.H.C.S.
13	C		1	INCONEL	
12	A		1	Al_2O_3	
11	B		1	Al_2O_3	
10	B		1	Al_2O_3	.250 O.D. x .125 I.D.
9	D/D	A	1	S,C	
8	C	A	1	S,C	
7	B	A	1	Al_2O_3	
6	C	A	1	S,C	
5	B	A	1	Al_2O_3	
4	B	A	1	Al_2O_3	
3	N.D.		12	S.S	1/4-20 HEX NUT
2	D		1	S.S.	
1	D	A	1	S.S.	

UNLESS OTHERWISE SPECIFIED

DECIMAL: .X ±.03, .XX ±.01, .XXX ±.005
FILLET RADIUS .010 MAXIMUM
THREADS: CLASS 2
⊚ DIA. CONC. WITHIN ___ T.I.R.
ALL OTHER DIA. CONC. WITHIN .005 ___ T.I.R.
SURFACES TO BE [illegible] WITHIN .001 ___ T.I.R.
SURFACES TO BE PAR. WITHIN .001 ___ T.I.R.
HOLE ANGULAR TOL. 0-2.0 RAD ±0° 5'
2.0-4.0 RAD ±0° 8'
ALL OTHER ANGULAR TOL. TO BE ±0° 30'
REMOVE ALL BURRS AND EDGES

SCALE: 2 X 1 | FINISH

495-1000

NEXT ASSY | SIMILAR TO

THERMO ELECTRON
ENGINEERING CORPORATION
85 FIRST AVENUE WALTHAM MASS 02154

DRAWN	CHECKED	ENGINEER
7/10/[illegible]		

TITLE:

Figure I-1

H | 562-1000 | 1 | B

FOLDOUT FRAME 6

An outer silicon carbide case, Part #9, received pre-heated hydrogen which, in turn, entered the diode region through a single ring of orifices drilled through the bottom of the oxygen cover and orifice plates.

The top of the oxygen orifice plate was attached to the exhaust tube, Part #41, which in turn carried the exhaust products to a three-stage recuperator, Parts #34, 35, 36, 37, 39 and 40.

A support ring, Part #54, was used to prevent movement of the exhaust tube relative to the outer case.

The oxygen manifold cover, Part #8, was covered with a layer of thin platinum to act as a radiation shield and reduce heat loss to the outer case.

The outer case was supported on cylindrical sleeves, Parts #4, 5, and 6, which in turn rested on a stainless steel plate, Part #1. The diode was supported from this same plate and was positioned concentric with the support sleeve. At the closest point the diode's hemispherical emitter shell was about 1/8 inch distant from the oxygen orifice plate.

Two spark ignitors, Parts M, were used. Each was driven by a neon bulb transformer.

A stainless steel hydrogen manifold, Parts #29, 30 and 31, was spring-loaded to the baseplate, Part #1, to hold the combustor together. A two-inch layer of thermal insulation enclosed all of the parts. Because the hydrogen-oxygen reactants might accidentally reach explosive proportions in the combustor, no outer case was employed. Any sudden increase in gas pressure due to burning was quickly and safely relieved by separation of the spring-loaded parts.

A thermal energy balance was conducted to establish the required fuel and oxidant flow rates and to properly size the various flow paths. This is described in the next section.

B. COMBUSTOR ENERGY FLOW

An energy balance was performed on the combustor design shown in Figure I-1. The results are summarized in Figure I-2.

The heat transfer by convection from the combustion products to the diode hemisphere was estimated by assuming a gas temperature of 3000°K and a diode surface temperature of 1600°K at the first ring of orifice holes, 1700°K at the second and third rings, and 2500°K at the fourth ring. A heat transfer coefficient of 15×10^{-3} watts/cm^2 °K was used for the 1600°K and 1700°K region and 7.5×10^{-3} watts/cm^2 °K in the 2500°K diode region. The resulting convective heat transfer was found to be 354 watts.

Heat transfer from the gases to the orifice plate, Part #6, was similarly estimated, using in this case a coefficient of 7.5×10^{-3} watts/cm^2 °K, and found to be 228 watts. Part of this heat was in turn radiated to the diode; this was calculated, assuming the average emissivity to be 0.76, and was found to be 158 watts. The remainder of 70 watts was radiated to the combustion chamber walls. A thin platinum shield was placed around Part #8 to minimize this component.

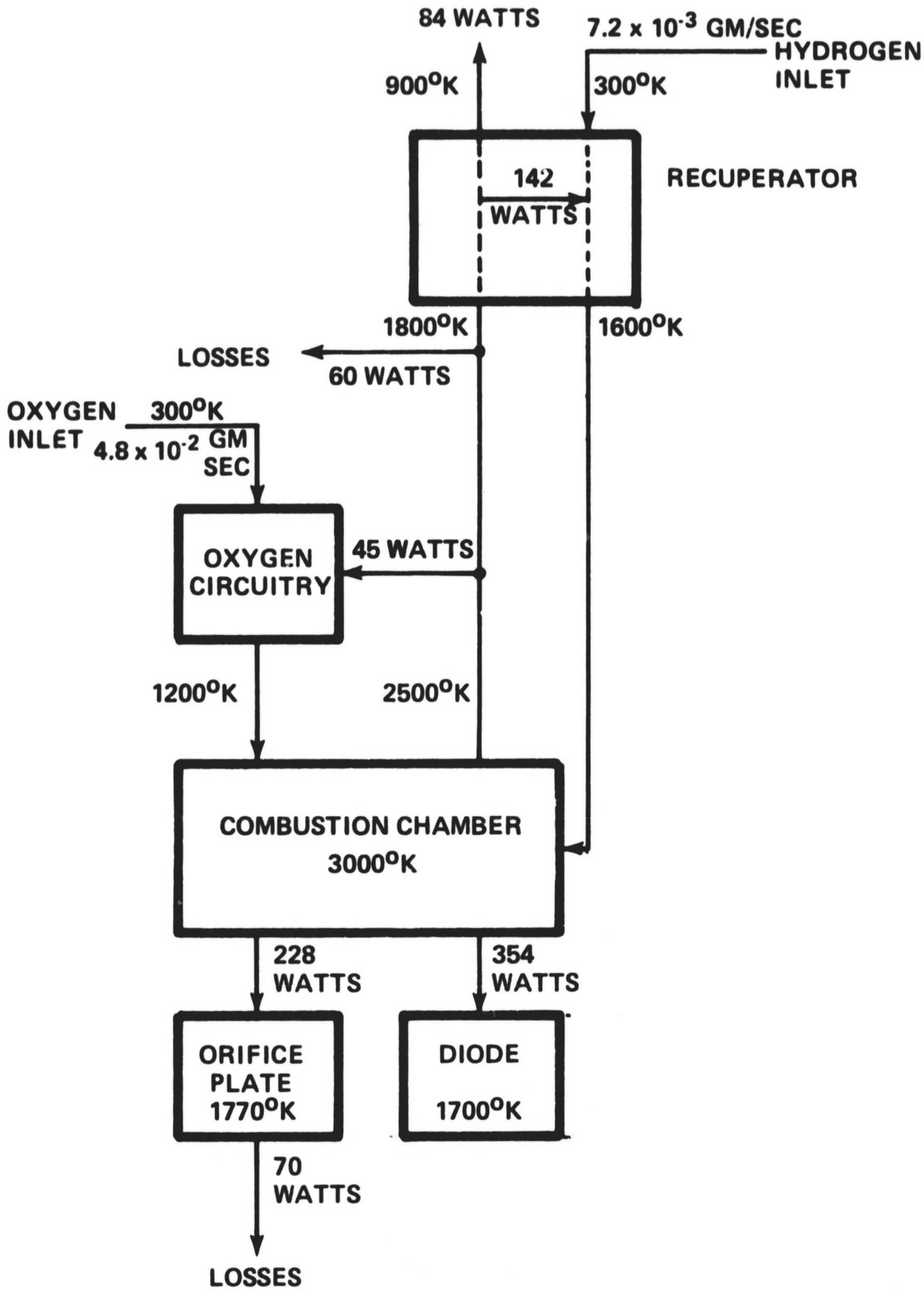

Figure I-2. Design Energy Flow and Temperature Distribution of the Combustor

The total energy extracted from the combustion products was the sum of that into the diode and that into the orifice plate, or 582 watts. Assuming that sufficient energy could be recuperated from the exhaust products to preheat the hydrogen to 1600°K, and assuming 20% excess hydrogen, the required hydrogen and oxygen mass flow rates were 7.2×10^{-3} gm/sec and 4.8×10^{-2} gm/sec, respectively.

Similarly, 45 watts was calculated to be the transfer from the combustion products to the incoming oxygen, raising the oxygen temperature from 300°K to 1200°K.

Approximately 60 watts was calculated to be lost to the environment through the insulation enclosing the recuperator section of the combustor.

The inlet and outlet temperatures of the recuperator on the exhaust product side were calculated to be 1800°K and 900°K, respectively, and 142 watts was transferred into the incoming hydrogen, heating it from 300°K to 1600°K.

The above energy balance assumed no leakage either between sections of the combustor or to the outside environment.

C. COMBUSTOR TESTS

For test, the combustor was first purged with helium. The spark ignitors were then energized and hydrogen flow was initiated. The hydrogen was ignited at the exhaust by a hot kanthol wire energized from the 60-cycle line with a variable transformer. Finally, oxygen was added and combustion took place in the diode region.

Figure I-3 shows the first combustor placed on test. A silicon carbide hemispherical shell (Figure I-4) was used to simulate the diode. The shell temperature was measured pyrometrically from below, i. e., from the side of the shell opposite the combustion region. At this time the recuperator prevented pyrometric temperature measurement on the combustion side.

When ignition was initiated, a series of sharp explosions was heard within the combustor. These were judged to be possibly due to air leaking into the combustion chamber; to avoid the possibility of a large accumulation of ignitable mixture in the chamber, two additional spark ignitors were added, as shown in Figure I-5. With this change, the combustor was reignited and the SiC shell was raised to 1330°C in several steps. Some exploding was still experienced during ignition. The hydrogen and oxygen flow rates required to reach 1330°C were far in excess of the design values; consequently, some experimentation with the recuperator was judged necessary.

The combustor was then reassembled with no recuperation, Figure I-6, with one stage, Figure I-7, and again with 3 stages, as in Figure I-8. In each of these three test configurations a tube was inserted vertically downward through the recuperator. This provided a means of viewing the combustion area during ignition, and a means for pyrometrically viewing the combustion side of the diode shell. Also, additional small sheets of thin platinum foil were placed in the combustion chamber in an attempt to catalyze ignition before a significant explosive

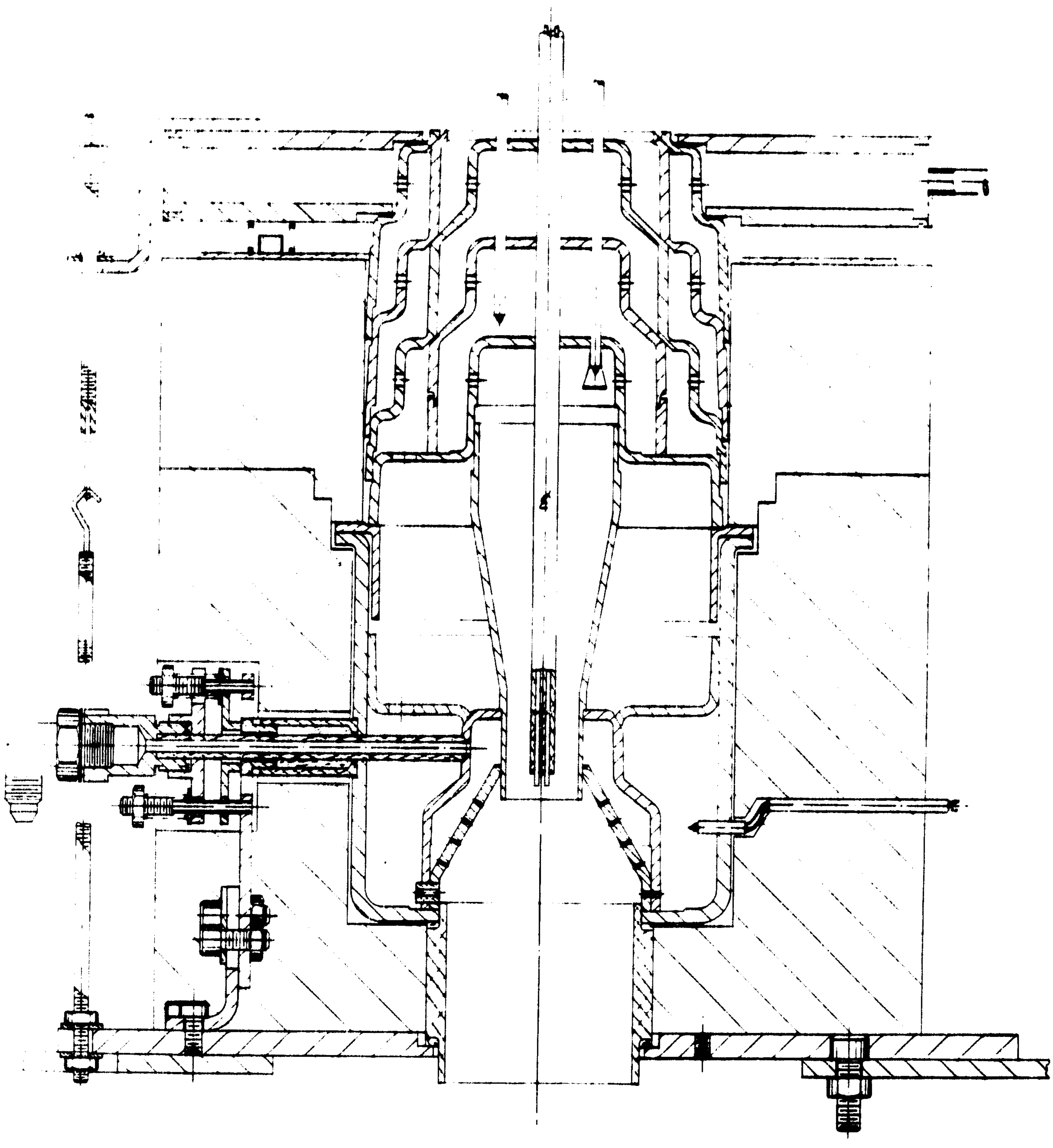

Figure I-3. Initial Combustor Design

Figure I-4. Silicon Carbide Test Shell.

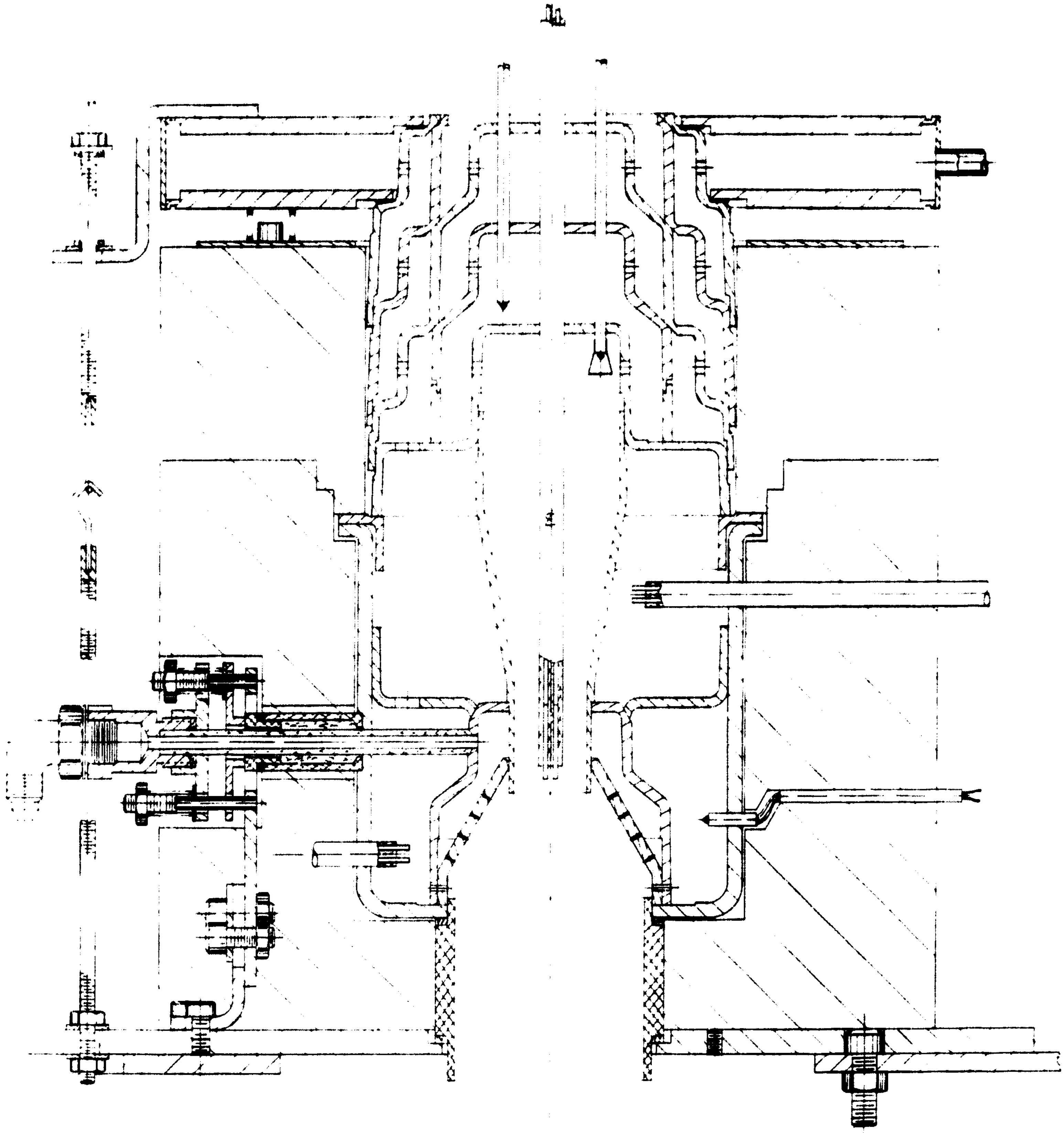

Figure I-5. Combustor with Added Spark Ingiters.

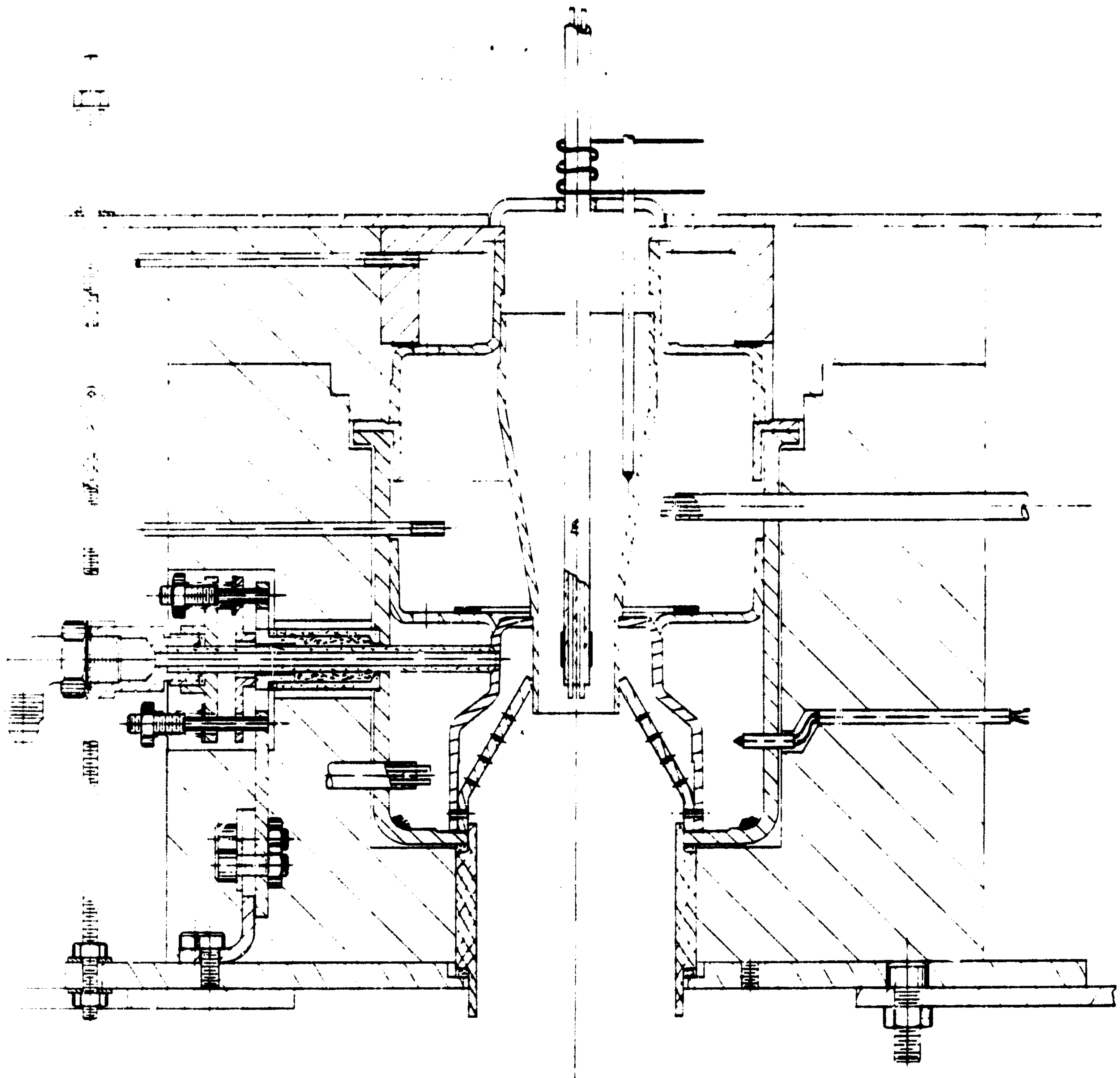

Figure I-6. Combustor without Recuperator

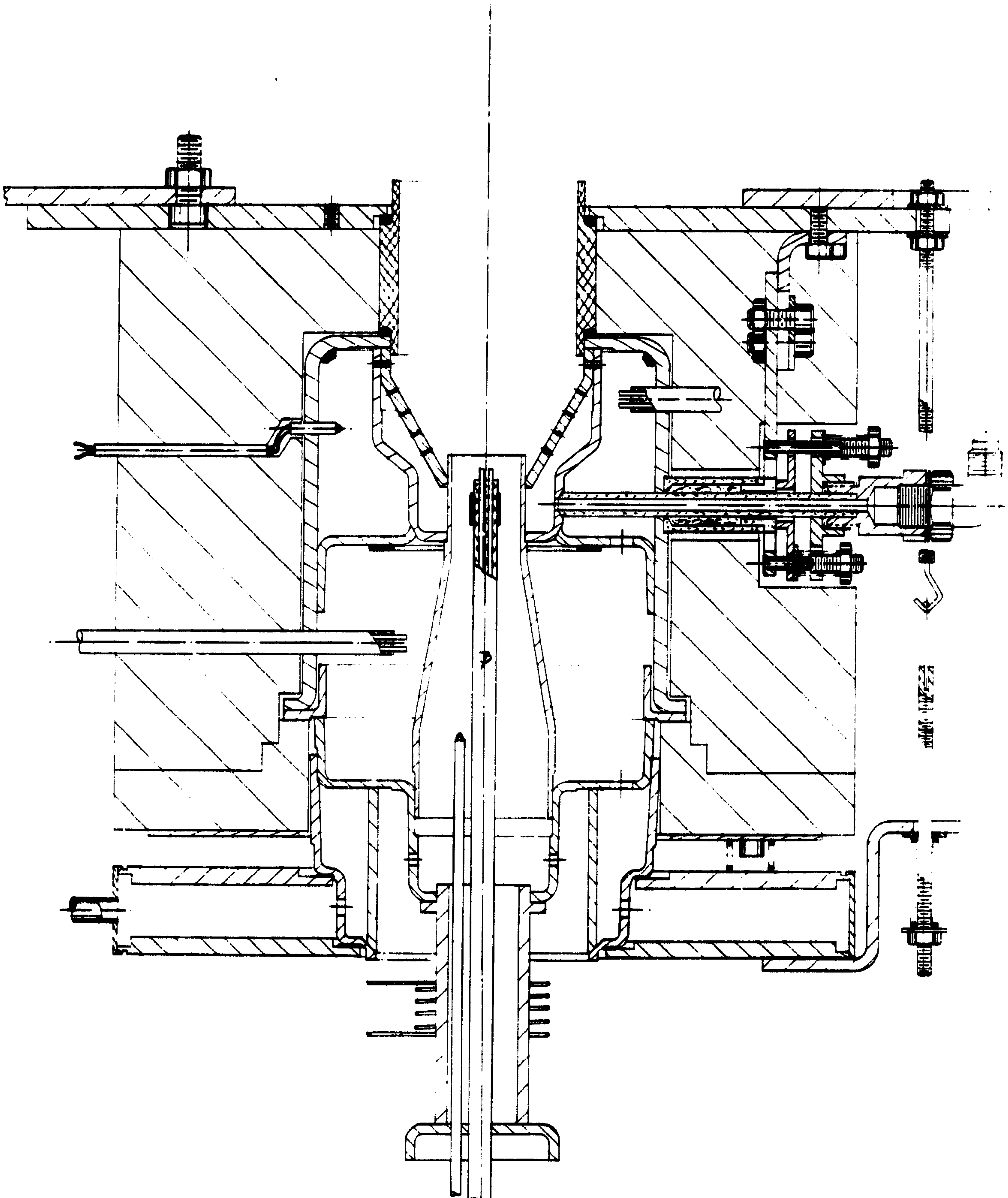

Figure I-7. Combustor with One Stage of Recuperation

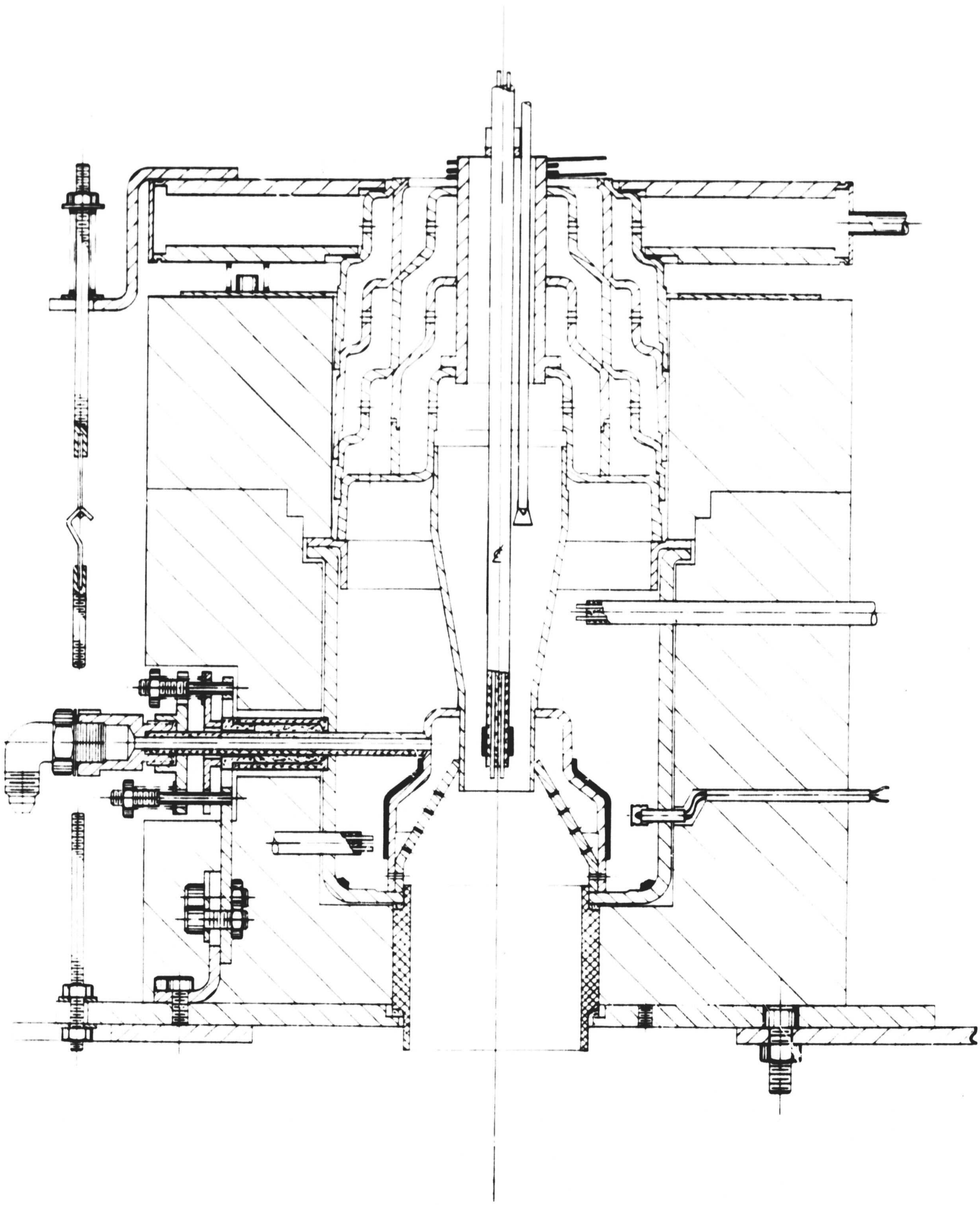

Figure I-8. Combustor with Three Stages of Recuperation mixture was formed and to thus reduce the popping during ignition. Changing the number of stages of recuperation had little effect, as did the addition of the platinum. The required hydrogen continued to be well in excess of the design values.

Leakage of hydrogen by permeation through the silicon carbide was an obvious possibility; consequently, in the next series of tests, the flow passages within the combustor were increased gradually in search of an optimization between heat transfer and leakage. As flow velocities decrease, heat transfer also drops, but lower velocities result in lower pressures and less leakage. Figure I-1 shows the resulting design that seemed to be the best compromise.

As the orifice sizes were increased, the best combustor performance, judged by the highest emitter temperature for a given fuel input, occurred at lower values of excess hydrogen. With the original configuration, over twice the stoichiometric hydrogen produced the highest temperature. With the final configuration, more nearly stoichiometric proportions were found optimum.

These results tended to confirm significant loss of hydrogen by permeation, probably through both the recuperator and the outer case. Good efficiency required sufficient flow velocities to achieve good convection heat transfer, and these velocities implied a pressure drop. The hydrogen permeation and the resulting fuel loss appeared excessive for acceptable heat transfer. Some means of reducing permeation while still retaining the ability to operate at high temperatures was needed. One possible solution was to make all the high-temperature parts from pyrolytically-deposited silicon carbide. Tests of the thermionic diodes, which employed this material as a protective shell, showed it to be strong, vacuum-tight, and impermeable. However, to accomplish this change required extensive development of deposition apparatus and was outside the scope of the program.

During disassembly of the combustor to add the exhaust tube, the oxygen manifold cover was found to be cracked. This self-bonded silicon carbide piece had been covered with a thin coating of pyrolytically-deposited silicon carbide to inhibit permeation of oxygen into the hydrogen manifold. The self-bonded material is relatively permeable. The cracking may have been caused by a difference in thermal expansion characteristics between the two types of silicon carbides. This suspicion was confirmed when a second, similar piece was heated in an oven and also cracked. An uncoated sample remained intact. Subsequently, only uncoated parts were used.

Figure I-1 also shows certain other design changes that were made to reduce heat loss. The support sleeve, made of self-bonded silicon carbide, Parts #4, 5, and 7 in this figure, was originally made in one piece. In the initial calculations, the conduction loss was estimated as 525 watts, assuming a thermal conductivity of 10.8 Btu/hr/ft^2 °F. Subsequent data indicated a much high conductivity of 60 Btu/hr/ft^2 °F, with a resulting loss of 3000 watts. To reduce this loss, the sleeve was cut into three sections separated by a fiber insulation; at the same time, the insulator between the sleeve and the stainless support plate was increased. A thin foil of platinum was used to cover the exterior silicon carbide parts.

As the flow passages in the orifice plate were opened and the velocities reduced, a more uniform temperature distribution was also observed on the diode shell. At the outset, there were sharply defined, high-temperature, circular zones opposite the orifices. During the later tests these circles could not be distinguished.

Figures I-9 and I-10 show the orifice plate, the oxygen inlet chamber and the exhaust tube assembly. Figure I-11 shows the complete combustor.

For safety, all tests were conducted in a special test chamber. A concrete block wall separated personnel from the combustor. The other side of the room had a wooden cover that was opened during testing to preclude the containment of high pressures in the test region.

Both hydrogen and oxygen were supplied from high pressure tanks through electrical switch interlocks that closed the inlet valves and purged the system with helium if either hydrogen or oxygen pressure dropped below a preset value. Neither hydrogen nor oxygen flow could be initiated without the ignitors operating.

To avoid the accumulation of pockets of hydrogen in the ceiling region of the room, two exhaust fans were kept continuously operating; reed switches automatically stopped gas flow and purged the combustor if a fan blade stopped turning.

The heat flow from the rear of the dummy shell is difficult to estimate accurately because the heat flow is partly by radiation, convection and conduction, and the view factor is uncertain. However, the assumption was made that radiation predominated and that the shell could be considered a radiating surface with an effective area equal to its cross-sectional area; on this basis, the burner efficiency was calculated for various shell temperatures. The results are shown in Figure I-12 for the final combustor configuration. Table I-1 summarizes burner data for several data points.

Table I-2 summarizes two generator data points where the system was carefully brought to thermal steady state.

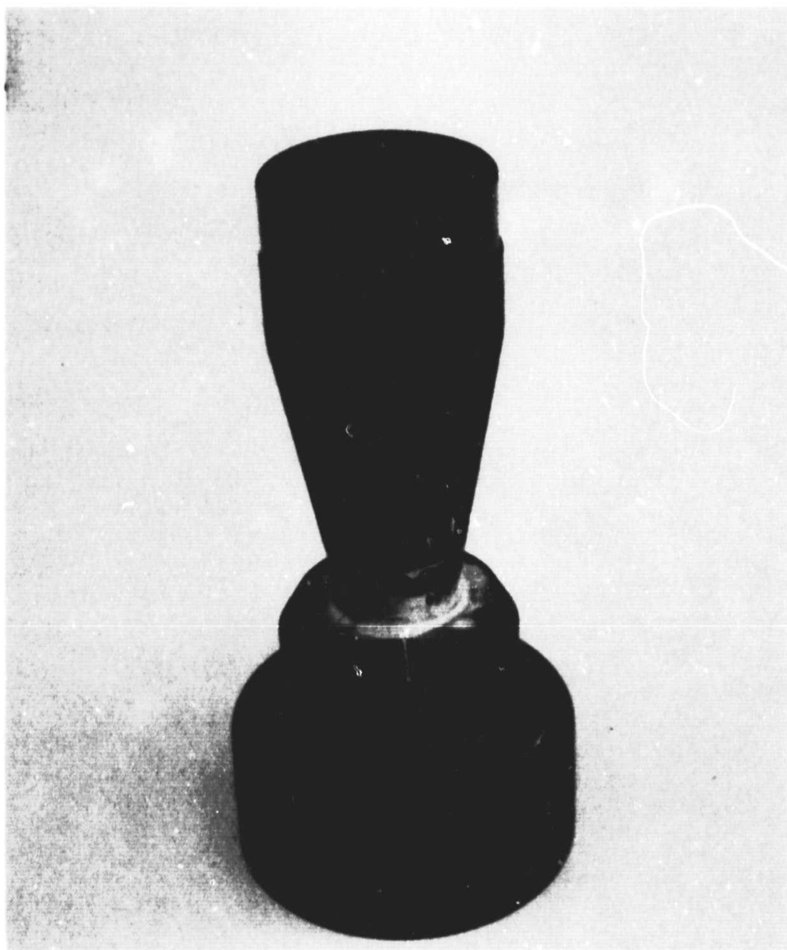

Figure I-9. Side View of Orifice Plate Assembly Showing Exhaust Tube at Top.

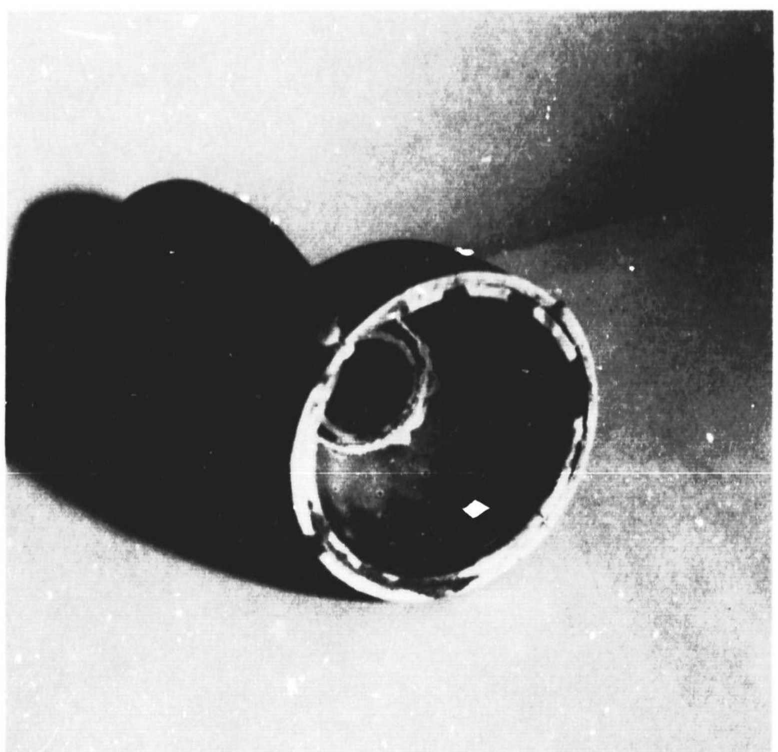

Figure I-10. Bottom View of Orifice Assembly.

8747

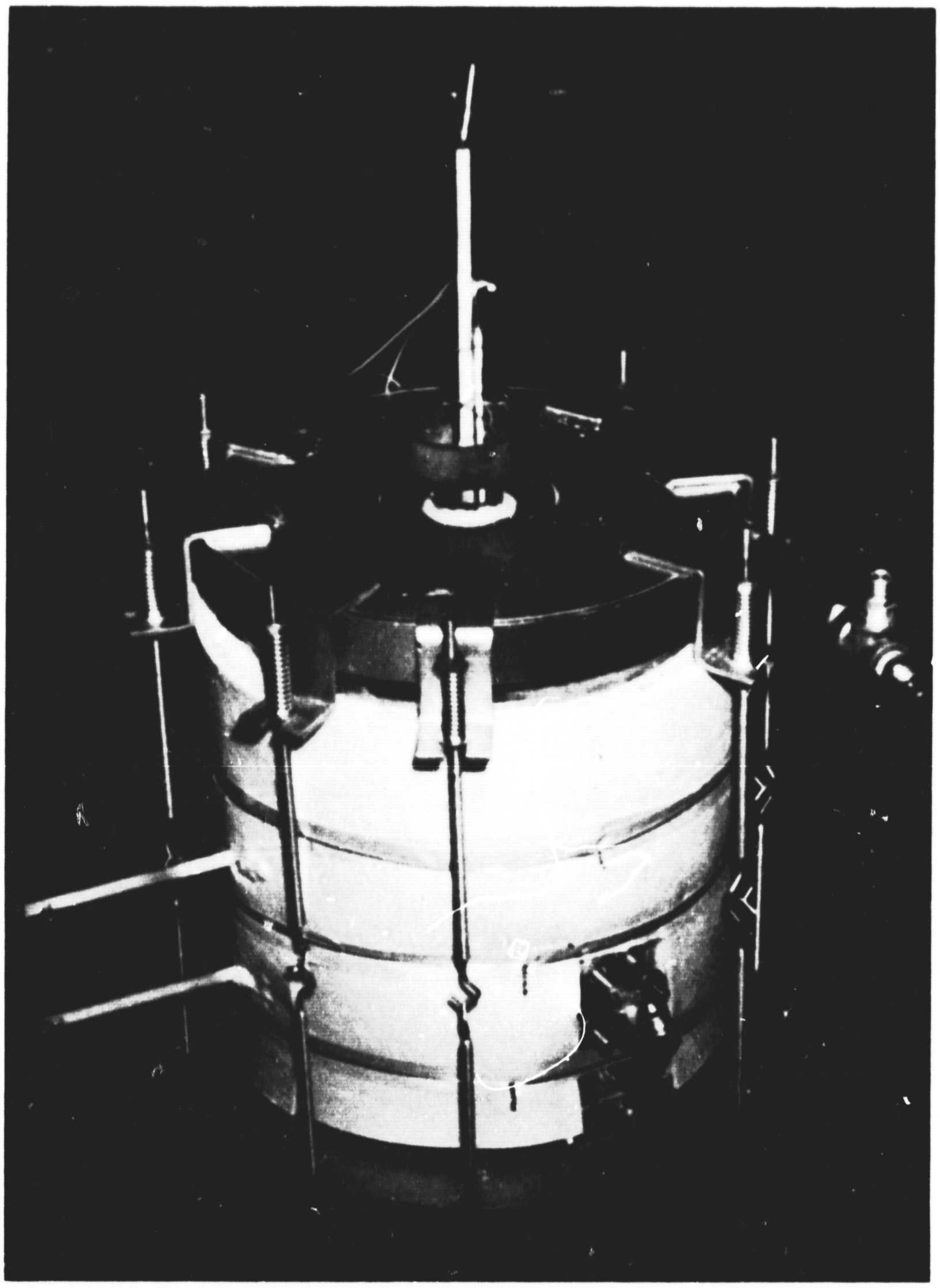

Figure I-11. Hydrogen-Oxygen Combustor.

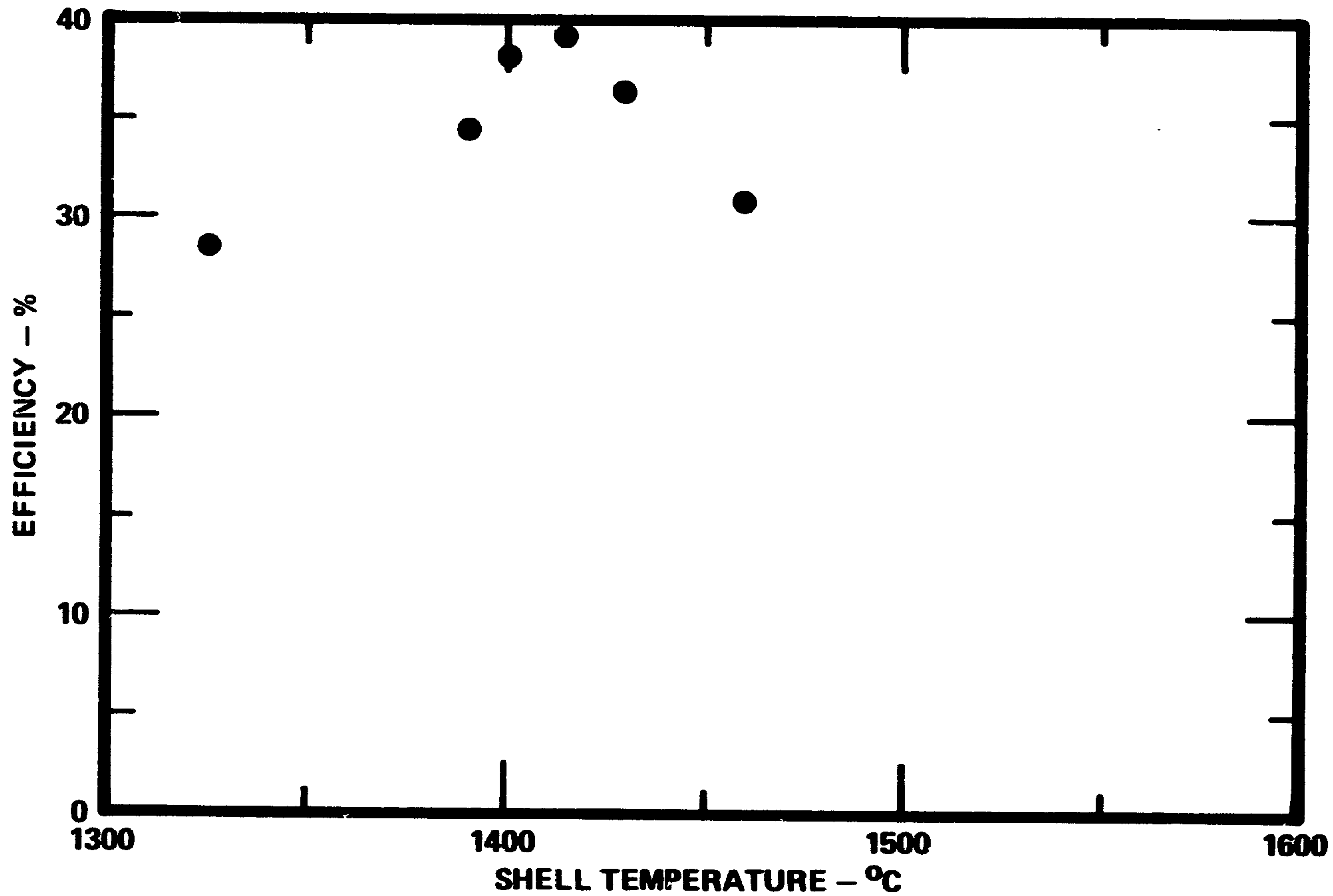

Figure I-12. Burner Efficiency versus Shell Temperature

TABLE I-1

TYPICAL COMBUSTOR PERFORMANCE DATA

Data Point	H_2 gm/min	O_2 gm/min	ΔP_{H_2} in H_2O	ΔP_{O_2} in H_2O	Shell Temp. °C
1	1.4	8.0	.15	NA	1455
2	1.26	8.0	.14	NA	1430
3	1.12	8.0	.13	NA	1415
4	1.12	6.9	.08	4.6	1400
5	1.2	5.8	.19	3.4	1325
6	1.2	6.2	.20	4.2	1390

TABLE I-2

TYPICAL GENERATOR PERFORMANCE DATA

Data Point	H_2 gm/min	O_2 gm/min	Shell Temp. °C	Diode Output Watts	System η %
1	1.61	8.4	1460	30.8	0.9
2	1.75	10.8	1450	38.7	1.04

II. FLAME-HEATED THERMIONIC DIODE

A. INTRODUCTION

The intent of the program was to deliver eight diodes essentially like those being developed by Thermo Electron on other programs, with the following changes:

1. All diodes were to use a heat pipe to transfer heat from the collector to the cooling fins in order to obviate the need for forced collector cooling.
2. Two diodes were to use a binary additive of cesium fluoride.
3. Two diodes were to have ruthenium emitters.
4. Two diodes were to have both ruthenium emitters and the cesium fluoride additive.

B. DIODE CONSTRUCTION

In this section, the method of constructing the diodes is described. Figure II-1 shows the diode in cross-section. The emitter shell is a tri-layer structure consisting of a tungsten emitter bonded to a layer of carbon which, in turn, is coated with silicon carbide. Both the tungsten and the silicon carbide are pyrolytically-deposited on a machined carbon mandrel. The tungsten was deposited from tungsten hexafluoride gas carried in a stream of hydrogen and the silicon carbide from methyl-trichlorosilane with hydrogen gas. The shell is brazed to a molybdenum flange that supports the diode in the burner and acts as an emitter electrical lead. An aluminum oxide insulator electrically isolates the emitter and collector. The collector

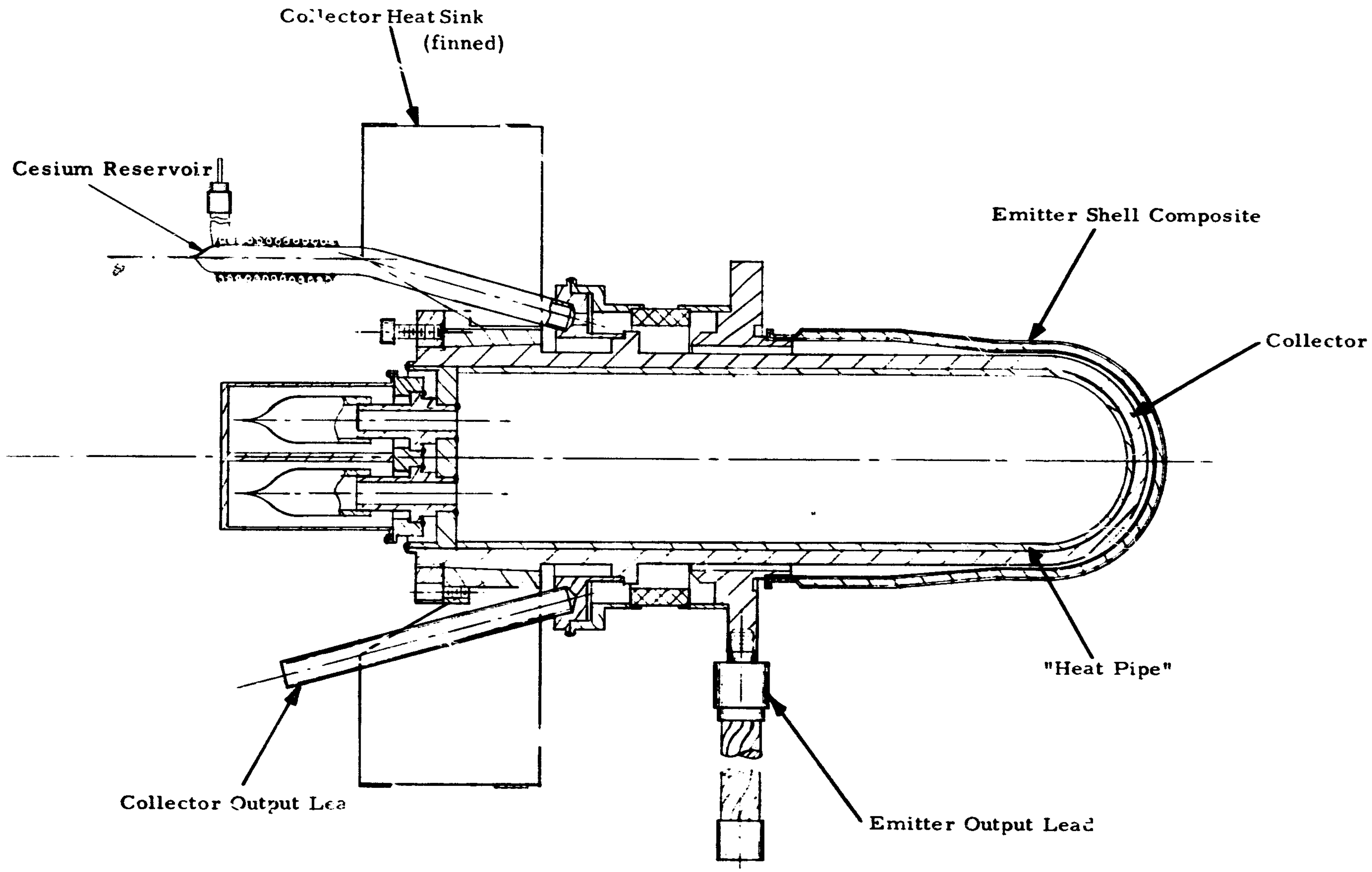

THERMO ELECTRON
ENGINEERING CORPORATION
65 FIRST AVENUE • WALTHAM, MASS. 02154

SK-574-12066
REV - B -

Figure II-1. Detail Drawing of Experimental Hydrocarbon-Fired Thermionic Converter, Series VI-S.

is cooled with the "heat pipe" principle and external fins. Figure II-2 shows a complete diode, and Figure II-3 shows the diode in an exploded view.

Diode testing at the outset was conducted on a methane-oxygen water-cooled burner shown in Figure II-4. All diode temperatures were recorded on a multipoint recorder except the emitter temperature, which was measured pyrometrically. Diode output was measured on a voltmeter and an ammeter. At first, a manually-variable resistance load was employed; later, a constant current load was substituted to allow better control. Electron cooling was a major heat load on the emitter, and the maintenance of a constant load current allowed much better control of emitter temperature. Cesium temperature was controlled automatically with an electronic temperature controller. Collector cooling could be varied during a test by covering a portion of the fins or by fan-cooling the fins. Provisions were made to automatically terminate burner operation if output power was lost or if the recorded temperatures exceeded preset values.

The first diode tested produced no output and was found to have a leak at the nickel pinch-off. Copper pinch-offs were used in subsequent diodes.

The second diode produced a maximum output of 95 amps at 0.36 volts, with an emitter temperature of 1400°C. The collector temperature was found not to be optimum and significant voltage drops were observed in the output leads. Collector cooling was varied by covering a portion of the fins. When the output leads were reassembled and improved, the bottom of the emitter shell

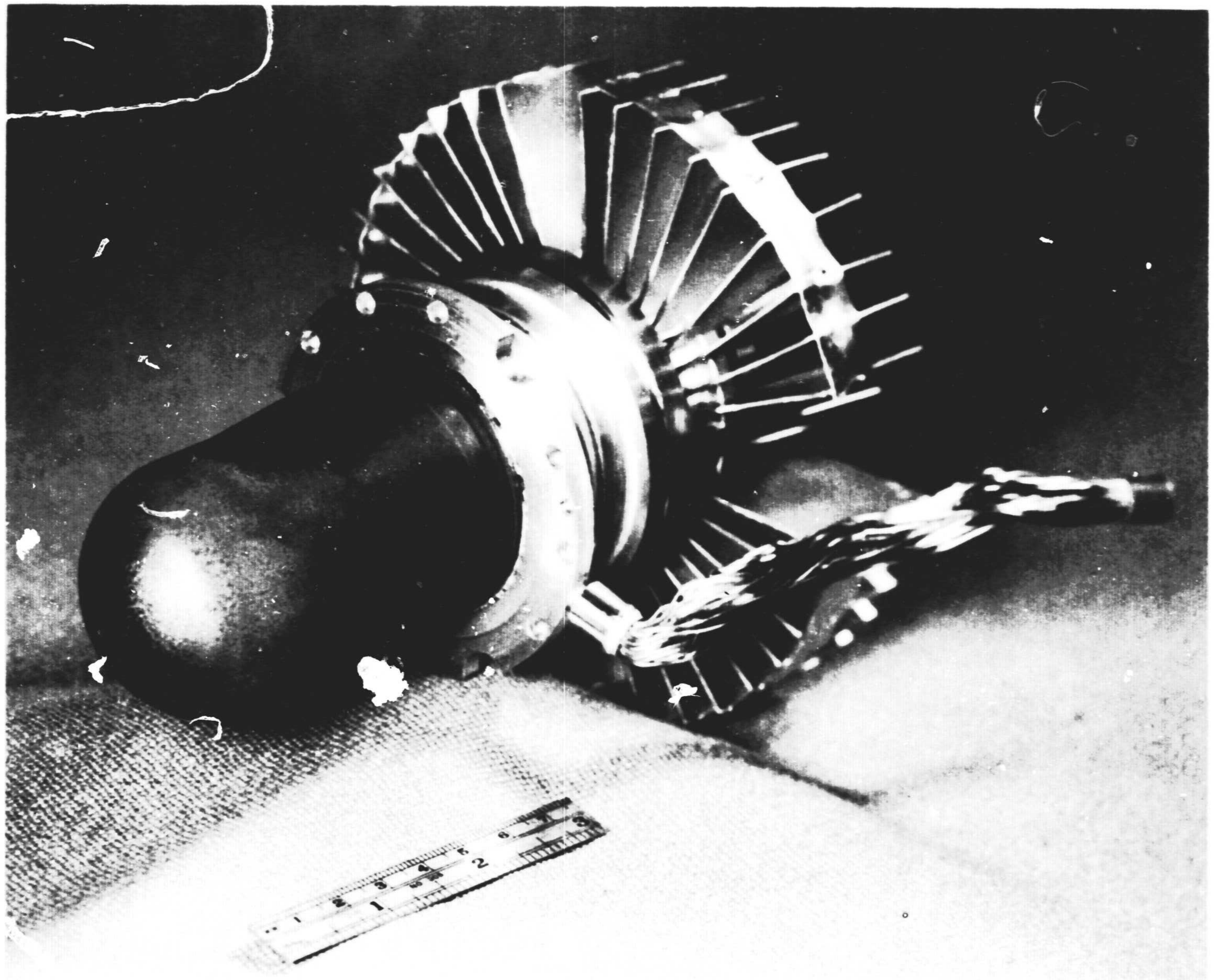

Figure II-2. Flame-Heated Thermionic Converter with Heat Pipe for Collector Heat Dissipation.

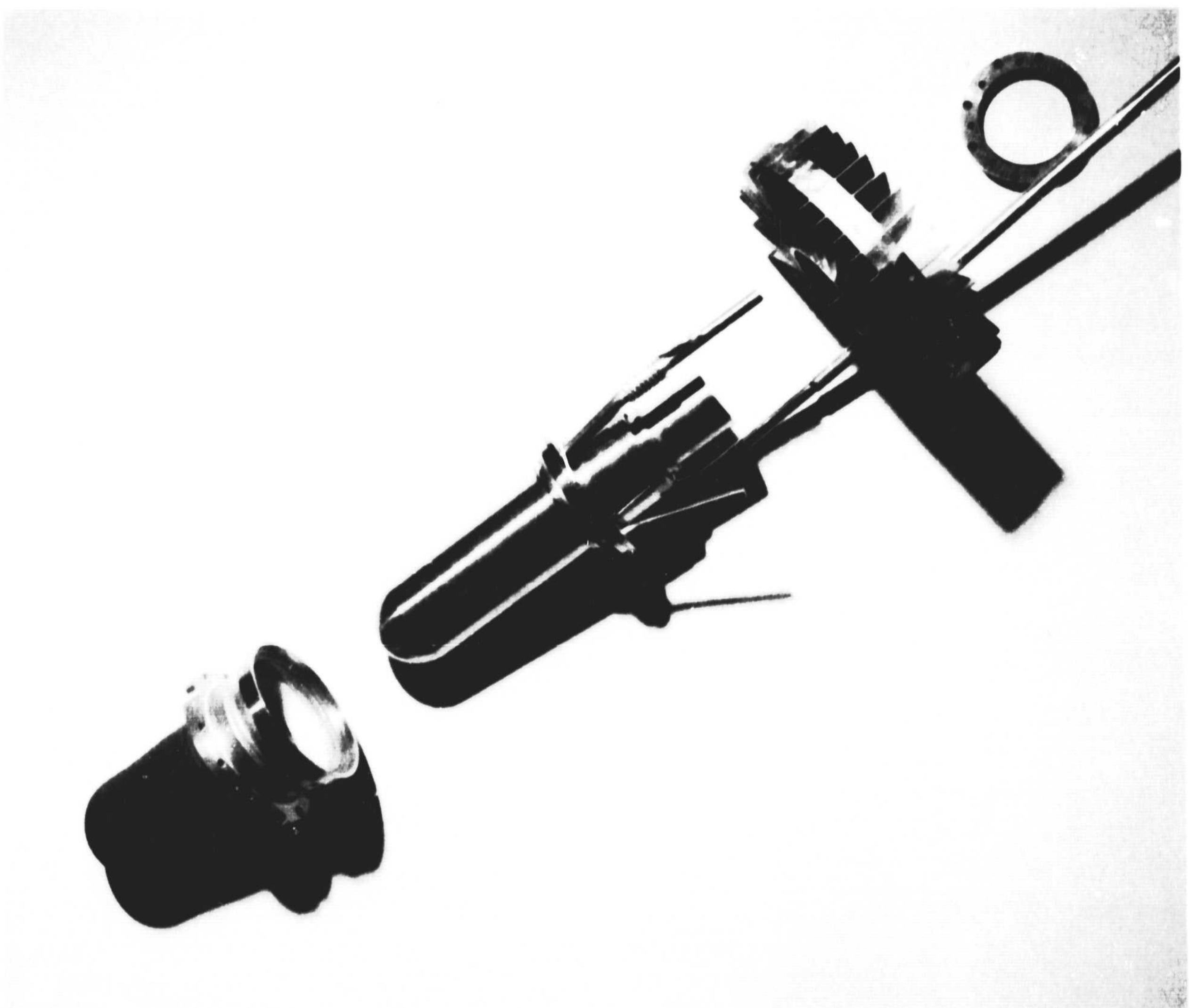

Figure II-3. Exploded View of Diode VI-S.

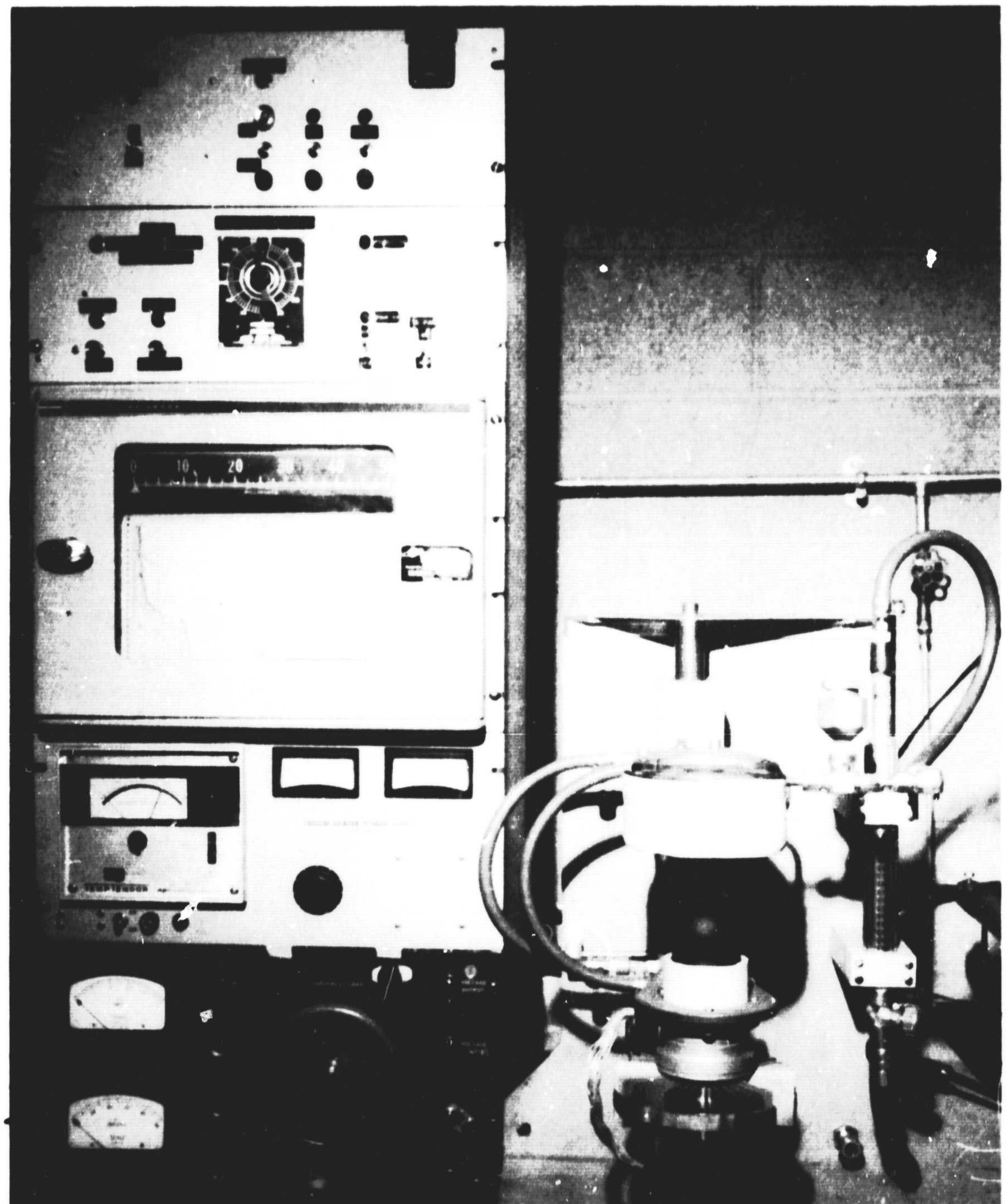

Figure II-4. Methane-Oxygen Burner.

dropped below a safe temperature, reducing the length of the emitter shell with respect to the collector and allowing the collector to touch the emitter. The collector cracked the emitter shell and output was lost.

The third diode constructed and placed on test was first operated in a methane-oxygen ring-type burner. Figure II-5 shows the output voltage and current at an emitter temperature of 1425°C. These I-V curves were obtained by scanning. In Figure II-6, the optimum envelope of the I-V curves has been converted into a power output versus output voltage curve. The emitter temperature varied widely over the hemispherical surface during the test. The 1425°C point recorded on these curves was measured pyrometrically in the region of the highest temperature on the side of the hemisphere. In the vicinity of the jets from the burner, the temperature was significantly higher than away from the jets. Furthermore, the temperature of the top of the hemisphere was considerably lower than that of the sides. Thus, it was difficult to establish an accurate emitter temperature. However, an attempt was made to read the emitter temperature consistently from diode to diode and from test to test. As can be seen from Figure II-6, the maximum power achieved by this diode was about 31.5 watts. This power output was significantly less than expected from a tungsten emitter of a surface area equivalent to the hemispherical surface and operating at an emitter temperature of 1425°C. Consequently, an effort was made to determine the cause.

Interelectrode spacing can affect significantly the power output of a thermionic diode. To determine the spacing of this diode, x-ray

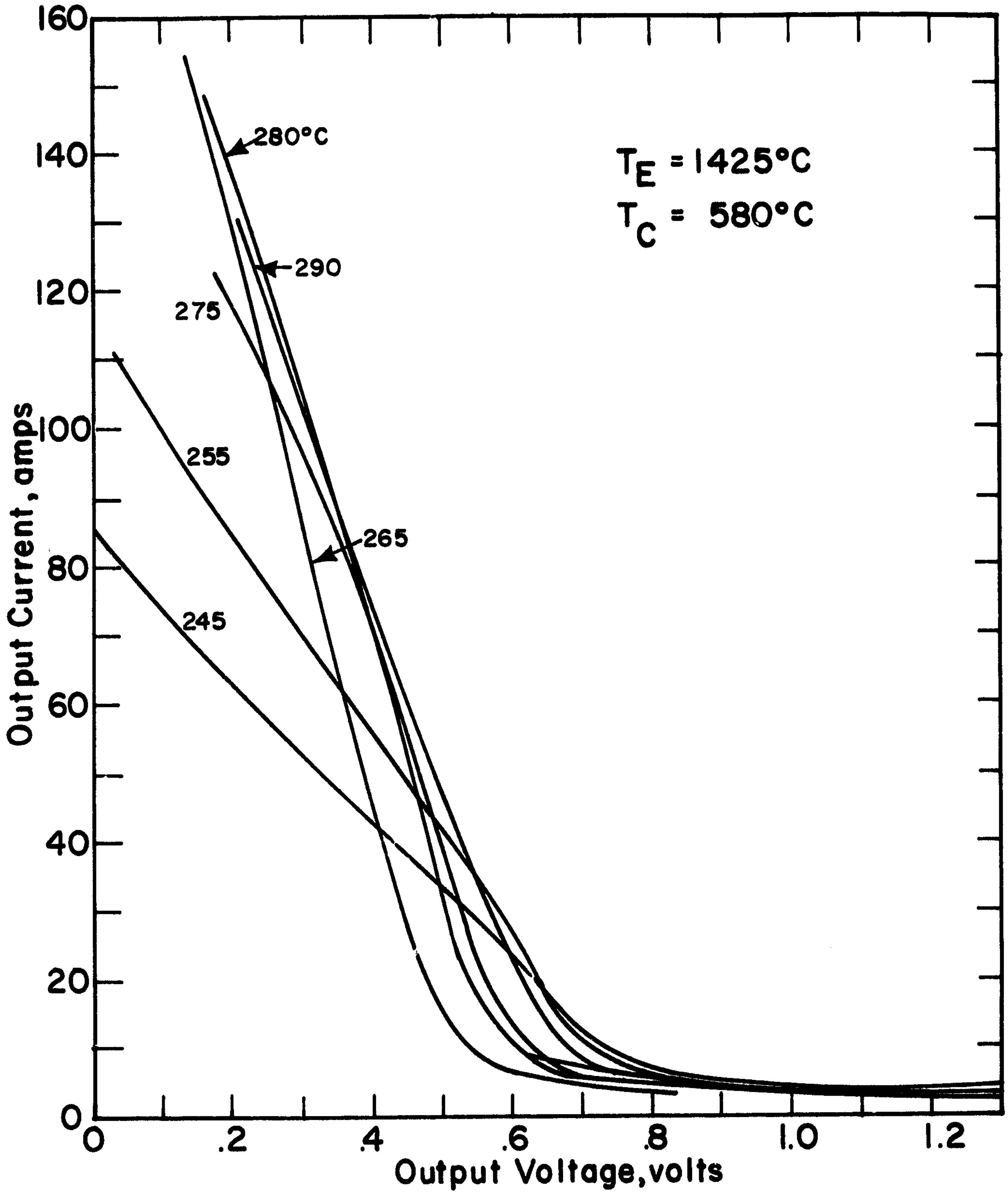

Figure II-5. Diode Current versus Voltage Output.

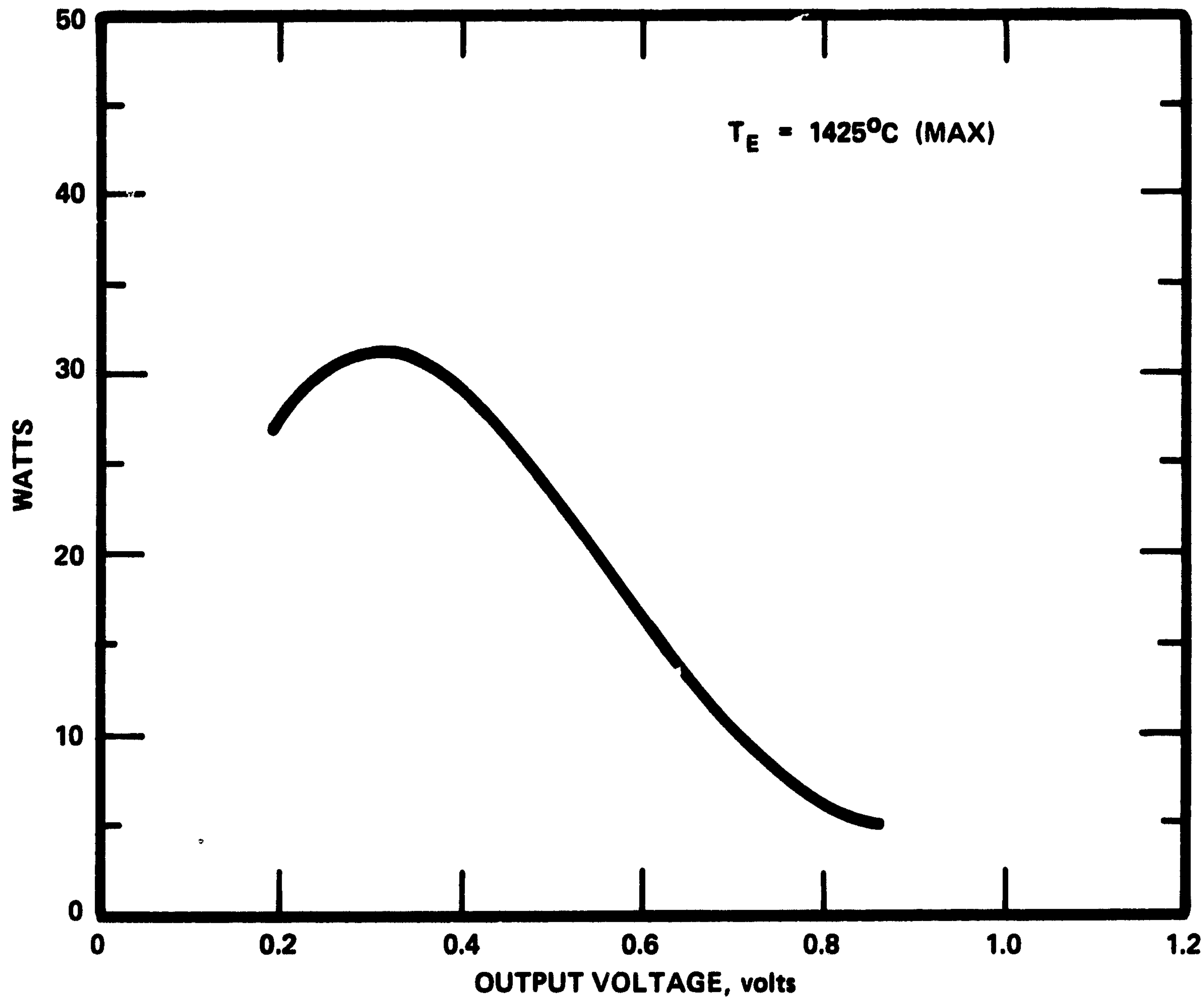

Figure II-6. Diode Power versus Voltage

examination was used. The interelectrode spacing was measured using several radiation levels to get an optimum definition of the emitter and collector surfaces, and was again found to be the cold design value of 26 mils. Next, diagnostic testing was conducted on the diode, trying to establish values for the emitter work function, the collector work function and the plasma losses. Unfortunately, the uncertainty in emitter temperature and the uncertainty in the amount of emitting surface made it virtually impossible to obtain definitive information from such diagnostic techniques. However, to the extent that these data could be interpreted, no significant deviation from the expected characteristics was observed. However, one very possible contribution to low performance could not be easily measured: the emitting surface may not have been completely clean of silicon carbide. During the deposition process, the inner portion of the shell was closed off by a plug at the bottom end to prevent silicon carbide from coating the tungsten surface. However, it had been observed that some silicon carbide did seep in. Prior to assembly of the diode, the emitter surface was lightly electropolished to remove as much of this as possible. In the next diode the amount of electropolishing was increased and some electroetching of the surface was added.

Following the test of diode #4, a fifth diode was immediately assembled. This diode incorporated additional electropolishing of the emitter surface; it was outgassed, cesiated, and placed on test. At an emitter temperature of 1350°C, this diode produced 50 amps at .35 volts. As the temperature was being raised to 1400°C, a discoloration of the emitter was observed in the form of dark spots randomly distributed on the hemispherical surface. Immediately the diode was open-circuited, due to fear that the collector had touched the emitter. (By open-circuiting the diode, the electron cooling was eliminated, thus cooling the collector and causing it to move away from the emitter. Also, by open-circuiting the diode, the emitter shell temperature increased, causing it to expand away from the collector). The diode was then cooled and examined; it appeared to still be in satisfactory condition. As a consequence, a second test was started. The diode was again raised to 1400°C, at which time a short was observed. This took the same form, namely, a series of dark spots appeared on the emitter shell. At 1400°C the output of the diode was 84 amps at .37 volts. At .35 volts, ignition of the diode had occurred at 50 amps. The diode was again open-circuited and allowed to cool down. On subsequent examination, it was observed that the silicon carbide in the hemispherical region had cracked. The diode was useless for further testing and, consequently, was opened and examined.

The examination indicated that the emitter surface had several small protuberances which extended away from the emitter by a distance of the order of 10 mils. In measuring the emitter shell dimensions for the purpose of fitting the collector, these protuberances had not been taken into account; consequently, the spacing in the region of these protuberances was much less than the average spacing. When the diode was taken up to temperature, the collector struck the protuberances, shorting the diode and eventually cracking the silicon carbide. To avoid this problem in the next diode, a special assembly jig was constructed.

Following the test of the fifth diode, several emitter-seal assemblies were lost during the final weld of the emitter and collector subassemblies. Specifically, the nickel inert-gas welds, which attach the heat pipe to the flange at the bottom of the seal structure, developed leaks to the atmosphere when the diodes were outgassing. In all cases, these leaks were large and sufficient air entered the diode to oxidize the interior of the emitter shell catastrophically. The ion pump was operating during this period for outgassing, but was not able to absorb the air as rapidly as it entered.

A careful microscopic analysis was made of a large number of nickel samples cut from the bars used for diode parts. Visually these samples appeared sound. Ultrasonic and X-ray analyses were also considered, but after discussions with experts in their use, these were deemed non-applicable at their present state of the art.

Next, sample pieces were fabricated from different bars of nickel, welded in inert gas, heated several times, and checked for leaks. These assemblies, constructed from parts cut from oversize-diameter bars, were found leak-tight. Removal of at least 1/2 inch of outer surface of the bar was deemed necessary to obtain sound welds with the nickel stock used. The procedure of using the oversize bar for these parts was then incorporated in the diode assembly procedure.

Concurrently with the studies of the nickel welds described above, similar welds were made in an electron-beam welder. These welds exhibited a behavior similar to that of those in the inert gas.

Nickel iron flanges were also evaluated as a back-up. These were completely unsatisfactory because of the development of leaks adjacent to the weld area.

Once a suitable welding technique was established, diode assembly was again undertaken. Two diodes were constructed, outgassed, and cesiated. One was tested, and produced 33 watts at 1400°C.

Up to this point the methane-oxygen test burner was always operated fuel-rich. In general, flame velocity is highest when burning stoichiometrically and recedes both in the fuel-rich and in the oxygen-rich sides of the ideal fuel-to-oxygen mixture. The flame velocity of the methane-oxygen combination was very high because there was no nitrogen to suppress the combustion, as there is in air. As a consequence, there was always concern that the gas flow velocity might drop inadvertently to a point where the flame would back up into the burner chamber, cause excessive pressure, and in turn result in an explosion of the burner shell. The burner system had flame arrestors upstream of the burner head and had a blow-off plug on the burner head to avert the danger of explosions. However, the shock from a back fire has been sufficiently sharp in one instance in the past to have blown out the plug and to have ruined a diode under test.

However, due to the necessity of expediting diode testing in order to deliver completed diodes, it was deemed necessary to experiment with running these ring burners in a more oxidizing regime. By doing this, it was expected that better combustion of the reactants as they leave the orifices and impinge upon the diode shell would be achieved, and, as a result, the diode could be driven to a significantly higher temperature. Experiments were run in which the burner was very quickly taken through the stoichiometric region and was then taken into the lean region. These experiments were successful, and operating in the lean region has resulted in the ability to run the diode at significantly higher temperatures. In this way, although the temperature distribution of the hemisphere is not uniform, an average temperature estimated at 1400°C can be achieved. As a result, this ring burner was used without further changes.

The sixth diode, which was constructed in the prior reporting period and produced 33 watts, was then placed on test in the ring burner with the new operative procedure; it produced 60 watts, indicating that the basic diodes were capable of meeting the performance requirements of the contract.

The seventh diode, when placed on test, performed very poorly and on subsequent x-ray was found to have a collector that was significantly eccentric with respect to the emitter shell. This eccentricity was deemed to be the result of tolerances in the machining of the collector assembly and a shift in the position of the assembly during the final weld. The problem had not been experienced before, even though a number of diode assemblies had been made, and a careful study of the jigging used during welding and the welding procedure indicated that the problem resulted from an extreme combination of tolerances.

Although a number of diode emitter and collector assemblies had been ready for final assembly, they were not committed to complete diodes, pending the testing of the sixth diode in a satisfactory burner to insure that it was capable of achieving the required power of 50 watts. Once this diode was tested and proved satisfactory, the diode design was frozen.

Two diodes were then constructed with polycrystalline tungsten emitters and two with etched tungsten* emitters. All four were heated in the methane-oxygen burner and shown to produce at least 50 watts at an average emitter temperature judged to be 1400°C and an output voltage of 0.35 volts. The diodes were operated for 12 hours in two six-hour test periods. Figure II-7 shows the diode ready for test, and Figure II-8 shows the diode operating.

Two diodes were also operated at 50 watts in a hydrogen-oxygen combustor.

Operation of the generator over the temperature range of -100°C to +125°C was not tested. However, the design is such that no difficulty in doing so was foreseen.

C. HEAT PIPE

The design of the prototype collector heat pipe is shown in Figure II-9. The pipe was machined from a solid bar of molybdenum. The hot end of this pipe is shown on the right side of the drawing and corresponds to the collector location. This collector end was .75 inch thick and had sufficient thickness to allow a hemispherical end to be machined. For the prototype tests, the collector end was left square to minimize machining cost.

---

*Described in Section II-5

8749

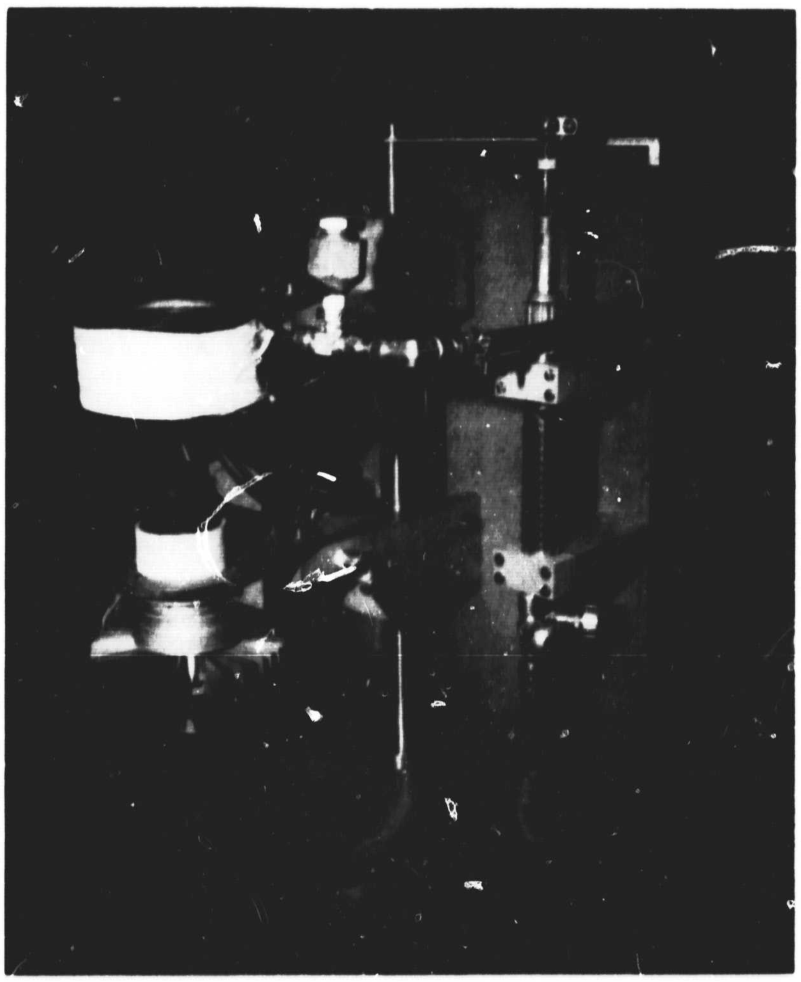

Figure II-7. Diode Installed in Methane-Oxygen Test Burner.

8750

Figure II-8. Diode Being Operated in Methane-Oxygen Test Burner.

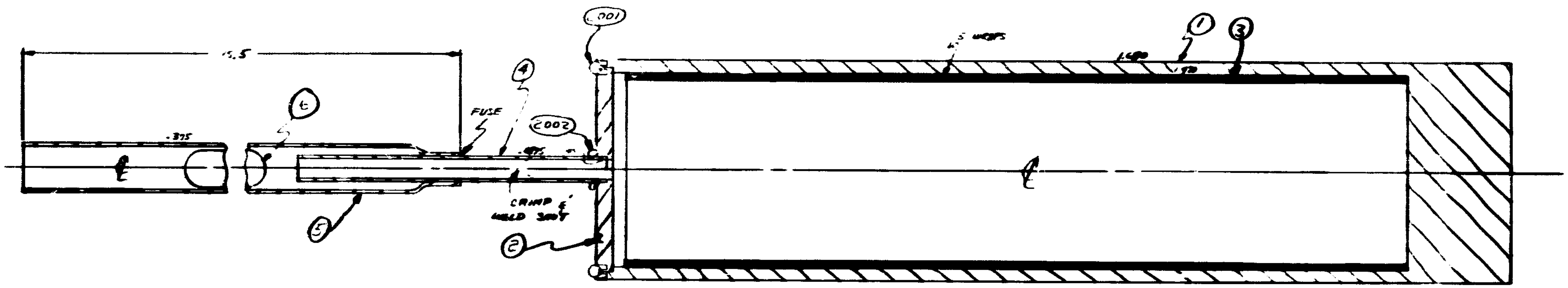

Figure II-9. Initial Heat Pipe Design

The capillary screen was inserted into the heat pipe through the cold end shown on the left side of the drawing. A molybdenum cap was then beam-welded over the end to close the pipe. A nickel tube penetrated this end cap to provide a port for the evacuation of the heat pipe and subsequent loading of the potassium working fluid.

A preliminary estimate of the potassium loading indicated that ten grams of potassium would be adequate for operation of the heat pipe, and ten-gram capsules were ordered. As received, these capsules consisted of 7 mm glass tubing of varying lengths with considerable oxidation evident on the inside of the capsule. Due to the long delivery period (approximately six weeks) the capsules were used for trial loadings.

Potassium loading consisted of a double distillation procedure to insure that high purity potassium was inserted into the heat pipe. The distillation rig included the glass potassium capsule, an intermediate distilling reservoir, and interconnecting copper and nickel tubing. The interiors of the heat pipe and the distilling rig were first outgassed at temperatures higher than the required normal operating temperatures. The glass capsule was then broken by squeezing the surrounding tubing, and the potassium was distilled into the intermediate reservoir. During this first distillation, the entire system was continually evacuated by means of a vac-ion pump to remove any gases liberated from heating of the potassium capsule.

With the potassium in the intermediate reservoir, the section of the distilling rig containing the broken glass capsule and the vac-ion pump were pinched off. The purified potassium was then distilled into the heat pipe. The reservoir was pinched off, a nickel cap was beam-welded over the final pinch off, and the heat pipe was ready for testing.

Since the potassium distillation rig was fabricated of all metal components, visual location of the potassium was not possible. Satisfactory potassium loading thus depended on the use of x-rays and the results of past experience. Initial efforts to distill the potassium were made at 300°C for periods of 24 hours. These conditions proved inadequate, and only partial transfer of the potassium was achieved. Subsequent trials at 400°C and times of about 12 hours were successful.

Experience showed, however, that some of the potassium was lost during the distilling process due to condensation in the evacuation lines and in the pinch-off tubes. Operation of the prototype heat pipe after the first successful loading using the ten-gram capsules showed that only the lower (or cooler) end of the pipe was operating as a heat pipe. The cause of this abnormal operation was believed to be a shortage of potassium. Twenty-gram potassium capsules were then obtained to insure that sufficient potassium was loaded into the pipe. The prototype was loaded with this quantity of potassium and initial tests indicated satisfactory operation.

More complete tests were then initiated to establish the performance of the test pipe. These showed that the heat pipe operated satisfactorily at low heat flux levels but could not achieve the 500 watt requirement of the diode heat transfer.

The premature heat flux cutoff experienced with the test pipe was ascribed to either an inadequate capillary liquid return system or an insufficient volume of potassium within the pipe. Considerable care has been taken in filling this pipe to insure that an adequate supply of potassium was available. However, it was difficult to establish with 100% certainty the exact amount of potassium in the pipe. In a second test pipe, further attempts were made to insure adequate filling. In particular, separate evacuation and charging tubulations were provided, and the potassium was singly-distilled directly into the pipe.

With regard to the capillary liquid return system, the pressure differential that the capillary system could support was a function primarily of the capillary tube diameter. It was possible that the capillaries were too large in diameter to generate the pressure required to overcome the head. As a consequence, another test pipe was constructed with smaller diameter mesh, namely, 200 mesh in place of 80 mesh. After outgassing, potassium was distilled into the heat pipe. In this case, a one-step distillation procedure was used, whereby the potassium was enclosed in a reservoir and directly distilled into the heat pipe while simultaneously pumping on a second evacuation tube to evacuate the pipe of any gases. After the distillation procedure was completed, the evacuation tube was pinched off. It was found that the potassium had distilled into the heat pipe and thence out of it and into the throat of the vacuum pump used for evacuation. This most probably occurred because the temperature of the heat pipe screen could not be lowered below the condensation point by the cooling strap attached to the outside of the pipe. A new cooling arrangement was designed.

The heat pipe containing the 200-mesh screening was then loaded and tested at nominal heat loads of 200, 300, 400 and 500 watts. The heat loads were monitored by a calorimeter located at the cold end of the heat pipe. Heat input was accomplished by means of an R. F. coil surrounding the hot end of the pipe.

The test configuration is shown in Figure II-10. The apparatus is shown in Figure II-11.

The test results are presented in Table II-1. The auxiliary heater was used to adjust the operating temperature of the cold end of the heat pipe. The power input was maintained at each value by maintaining the R. F. input constant.

The data in Table II-1 showed that the heat pipe could handle 500 watts with a temperature drop of 150°C. This met the diode requirement. Although the molybdenum heat pipe operated adequately, it became apparent in the diode design that the use of nickel was advantageous because it minimized the possibility of the emitter striking the collector during cool-down. Nickel has a much higher expansion rate than molybdenum and would contract more rapidly on cool-down than would molybdenum. Nickel had also been mentioned in various articles and literature as having more desirable thermionic properties than molybdenum. A new heat pipe using nickel rather than molybdenum was designed, assembled and tested.

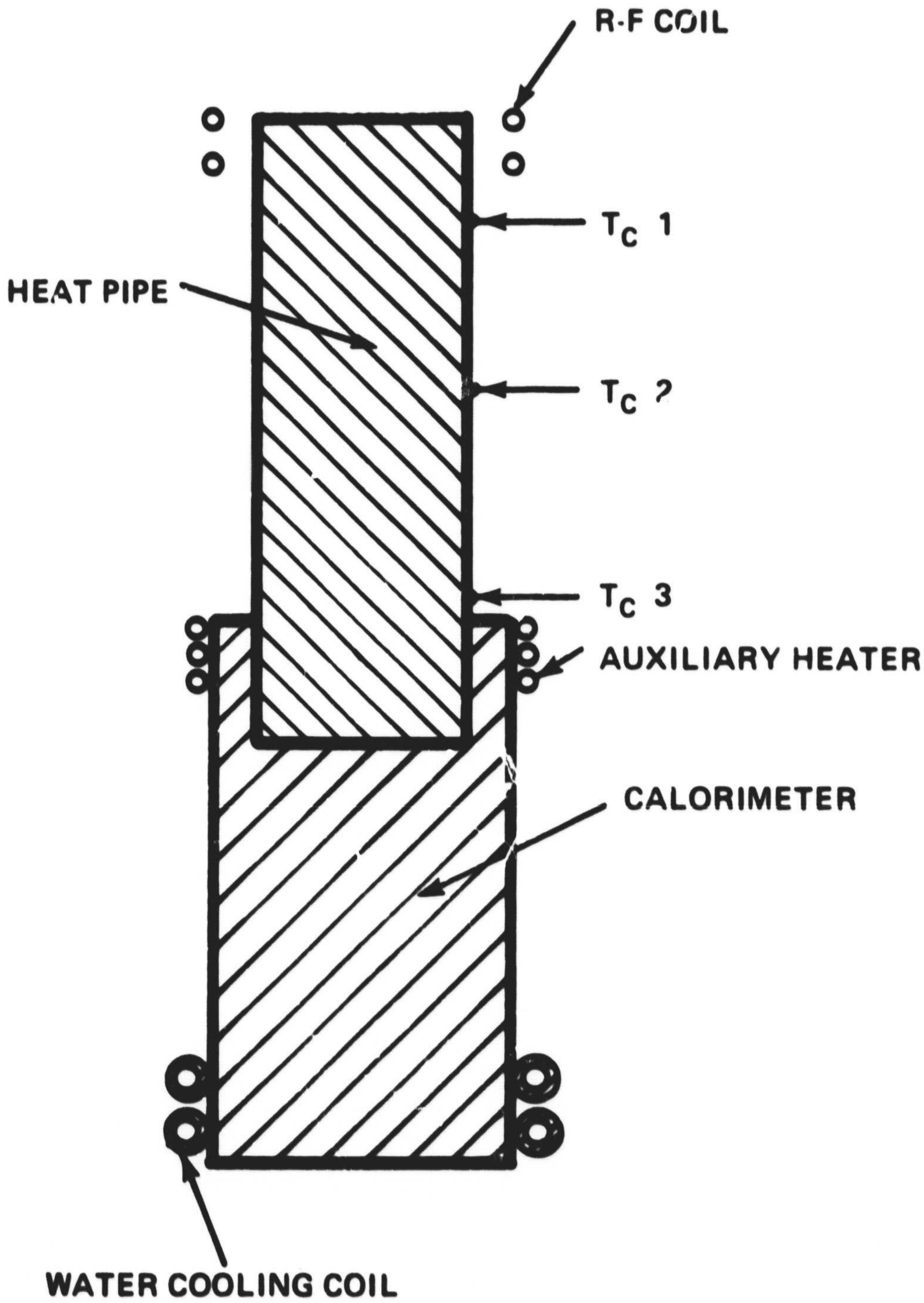

Figure II-10. Heat Pipe Test

8751

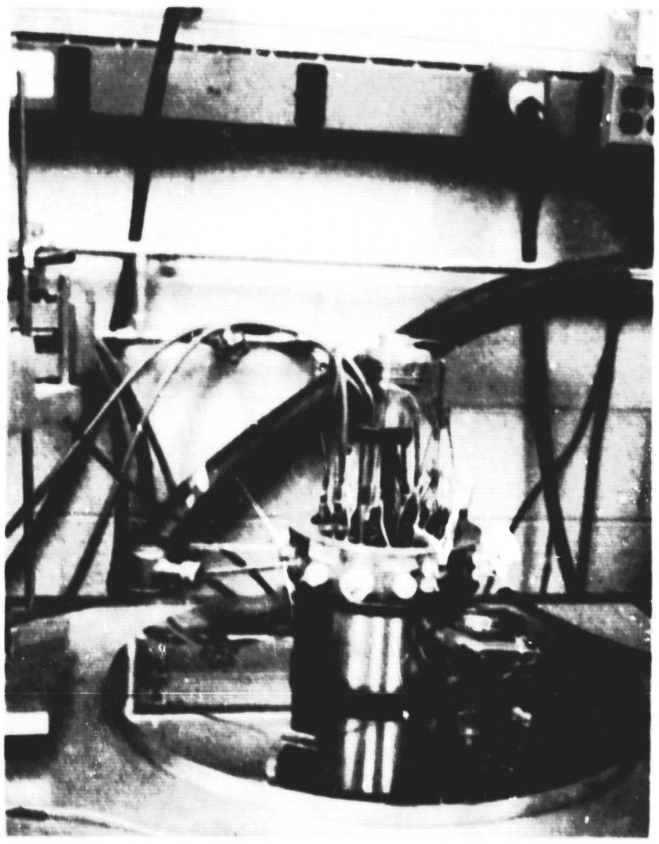

Figure II-11. Setup for Calorimetric Measurements of Heat Pipe.

TABLE II-1

HEAT PIPE TEST RESULTS

Normal Heat Load (Watts)	Thermocouple Temperature (°C)					Auxiliary Heater (Watts)
	T_C #1	T_C #2	T_C #3	T_C #4	T_C #5	
200	441	438	324	177	45	0
	459	457	423	234	56	100
	500	497	485	290	65	200
	541	539	530	332	71	300
300	495	474	438	229	56	0
	600	520	504	266	62	100
	620	552	539	325	47	200
400	678	560	544	280	64	0
	678	563	548	319	67	100
500	745	610	595	319	67	0

Table II-2 below summarizes the performance at various levels of heat flow.

TABLE II-2

HEAT PIPE PERFORMANCE

Temperature at Top (where heat is applied)	506	552	653	754	752	881
Temperature at Bottom	504	550	647	748	740	856
Q, watts	260	310	475	525	545	650

As can be seen, the temperature drop was very small over the entire range. This pipe utilized 200-mesh stainless steel screen supported by one layer of 80-mesh stainless steel screen. The upper portion of the heat pipe was hemispherical and the mesh had been formed in the hemispherical shape of the collector. This heat pipe was then available for incorporation in a diode.

D. ADDITIVES

At the outset the program plan called for use of a cesium fluoride additive in four diodes. Shortly thereafter, research results* showed that the performance improvement experienced with this additive was probably due to small amounts of oxygen from water vapor injected with the cesium fluoride. The program plan was then changed to substitute oxygen as the additive.

Copper oxide was judged a suitable dispenser of oxygen. To examine the possibility of evaporation of copper from the copper oxide additive used in a diode and its possible deposition on diode components, a test was performed in which the temperature and

*Final Report, Thermionic Research Program; by Kitrilakis et al; August 1966; Contract 951262; Prepared by Thermo Electron Corporation for Jet Propulsion Laboratory, Pasadena, California; Report No. TE 12-67.

geometries prevailing in a diode were reproduced The copper oxide was sintered in the form of a cylindrical pellet, which was inserted in a block simulating the collector. The copper oxide cavity communicated with the interelectrode spacing through a .010" orifice. An emitter was placed over that collector at a distance of .005". The objective of the test was to establish whether copper deposits would be detected on the emitter or the collector surfaces after 24 hours of testing under conditions prevailing during the operation of a converter. The emitter temperature was maintained at 1300°C with the collector temperature at approximately 750°C. The temperature of the emitter was measured with an optical pyrometer, while the temperature of the collector was measured through a chrome alumel thermocouple. After the test, the surfaces of both emitter and collector were examined, but no traces of copper and no discoloration could be detected.

A complete flame-fired diode, in which three copper oxide pellets were placed around the collector stem near the seal, was then constructed. Thin metal covers were spot-welded to the collector to hold the copper oxide. During the first test, one of these covers separated from the collector and shorted the diode. no useful test data was obtained.

At the same time, various research test results on other programs showed that lengthy and detailed experimentation was necessary to establish a suitable means of dispensing oxygen in a diode. The copper oxide method was shown to be unsuitable, amongst other reasons, because of the decomposition of the oxide into other corrosive compounds before oxygen was released. Such research was beyond the scope of this program and further efforts to include additives were terminated.

E. EMITTER PREPARATION

At the outset, the program called for the use of ruthenium emitters on four diodes. However, as in the case of the use of additives, extensive research underway with various emitter materials indicated that a specially-prepared tungsten emitter should result in better performance.

Two diodes were constructed and delivered with specially-etched tungsten emitters. Various electronic test equipment was substituted for the remaining two diodes.

The method of preparing the emitters was determined experimentally by etching samples and comparing these microscopically with etched emitters that had been tested in planar diodes. The best approximation was obtained by etching in the following electrolyte for 30 seconds at a bath temperature of 70 to 80°C:

30 cc, HF

10 cc, HNO_3

40 cc, H_2O

This method was used to prepare the two emitters.

III. GENERATOR MOCK-UP AND TEST CONSOLE

A non-operating mock-up of the complete generator was designed, constructed, and delivered. A test console was also designed for evaluation of the generators. Wiring and plumbing diagrams and a parts list were prepared and delivered. These were subsequently revised to incorporate changes shown desirable by the generator testing. The revisions were described in a separate communication which also included a suggested operating procedure.

IV. TEST EQUIPMENT

The following pieces of test equipment were delivered:

1. A diode test stand and burner
2. A constant current power supply
3. A high current power supply
4. Three stainless steel calibration loads

In addition, a sampler and recorder supplied by MSC were repaired for use in diode testing.

V. CONCLUSIONS AND RECOMMENDATIONS

The purpose of this program was to evaluate the state of the art of thermionic hardware for use in a mission of short duration (a few hours to a few days) to efficiently produce electric power with hydrogen and oxygen as the reactants. Clearly, this effort has shown that a much less permeable high-temperature material is needed for the combustor. Silicon carbide of the self-bonded or pyrolytically-deposited type is the only material that seems capable of withstanding both the high temperatures in the combustor and the thermal shock of starting and stopping the generator. Basic development effort is needed to find ways of making all of the parts with the impermeable, pyrolytically-deposited silicon carbide or to find a way of coating the self-bonded type with a pyrolytically-deposited layer where the combination has sufficiently similar expansion characteristics to avoid cracking.

When such a material becomes available, the basic design approach used in this first combustor should result in high efficiency. It remains to be seen whether the parts can be made in thin sections to also achieve low weight.